Title
Small molecule membrane transporters for enhanced microbial production of biochemicals

Author
Boyarskiy, Sergey

Publication Date
2015

Peer reviewed|Thesis/dissertation

Small molecule membrane transporters for enhanced microbial production of biochemicals

by

Sergey Boyarskiy

A dissertation submitted in partial satisfaction of the

requirements for the degree of

Joint Doctor of Philosophy
with University of California, San Francisco

in

Bioengineering

in the

Graduate Division

of the

University of California, Berkeley

Committee in charge:

Professor Danielle Tullman-Ercek, Chair
Professor Kathleen Ryan
Professor Hana El-Samad

Summer 2015

Abstract

Small molecule membrane transporters for enhanced microbial production of biochemical

by

Sergey Boyarskiy

Doctor of Philosophy in Bioengineering

University of California, Berkeley

Professor Danielle Tullman-Ercek, Chair

Metabolic engineering has been applied to a variety of microbial hosts to enhance production of compounds spanning from biofuels to pharmaceuticals. In all cases metabolic engineering requires the identification and optimization of the production pathway; however, engineering of optimal host strains capable of reliable production is multi-layered and complex. Strain engineering beyond the primary conversion pathway can lead to improved production levels, more robust strains, and better compatibility with downstream recovery methods. A common area where this facet of strain engineering becomes important is in alleviating the encumbrance on the cell caused by high product concentrations. In particular, these concerns are most relevant where productivity has to be maximized to achieve economic value, such as in commodity chemical and biofuel production. Many of the compounds valuable on an industrial scale are solvent-like hydrocarbons, where the accumulation of the compound is toxic to the cell. Furthermore separation of the somewhat hydrophobic compound becomes difficult as the large scale of the product formation leads to dissolved cell contaminants in the final product.

One potential engineering platform – efflux pumps – addresses many of the difficulties that come about from increased product yields. Engineered efflux transporters can secrete the product from the host thereby eliminating any potentially unwanted interactions between the product and the entirety of cellular machinery. Furthermore, secretion serves as a preliminary purification step for those compounds that are easily miscible with the rest of the cellular environment. This work discusses advances in the use of native and engineered efflux transporters to increase biochemical productivity. To this end, our first approach was to utilize directed evolution to mutate the native *Escherichia coli* efflux transporter AcrB to secrete the biofuel butanol. While AcrB's native function is mainly in stabilizing *E. coli* tolerance to bile salts and antibiotics, we were able to alter its specificity towards *n*-butanol and other short, straight-chain alcohols. We managed to increase tolerance of the cells expressing these mutant pumps to butanol as well as increase titers of butanol when the production pathways were added into the strains.

In addition to demonstrating that directed evolution approaches can be used to enhance secretion of toxic products from the cell, we developed a continuum kinetics model of transporter activity and molecular diffusion of small molecules across the membrane. An interesting conclusion of this model shows that efflux transporters are

likely to have the most benefit in the secretion of more hydrophilic molecules. However, when the model is expanded to include phase formation and separation of highly hydrophobic molecules, a new function for transporters is found. Transporters acting on very hydrophobic molecules are theoretically capable of creating a gradient strong enough to drive phase formation outside of the cell while keeping cellular concentration of the molecule at or below saturation concentration. Using this insight we searched for and identified native pumps in *Saccharomyces cerevisiae* capable of secreting the biodiesel molecule farnesene. Inactivation or deletion of these pumps results in intracellular accumulation of farnesene during production or from exogenous addition of the molecule.

This thesis serves as a foundation for developing the tools and for study and application of efflux pumps in biochemical production platforms. Our model, supported by empirical findings, can be used to help in the search of native transporters with unknown substrate specificities, and the tools we developed in engineering AcrB can aid in expanding the metabolic engineer's toolbox for high yield chemical production

Table of Contents

List of Figures

Acknowledgments

I would like to thank all the people that made the execution of this work a lot more enjoyable and fulfilling. Firstly, I'd like to thank my PI and mentor Danielle Tullman-Ercek. Danielle, thank you for taking me as your student and offering the guidance I needed to complete my Ph.D. You have always provided me with just the right mixture of freedom and oversight to let me explore the questions I was interested in without straying too much. You gave me a place to grow as a scientist, and for that I am forever thankful. In addition, I would like to thank the other faculty that had given me great advice and space in their labs during my tenure at UC Berkeley: Clayton Radke, Adam Arkin, J. Chris Anderson, and John Dueber.

I extend my thanks to the rest of the Tullman-Ercek lab. Without exception, each one of you gave me inspiration and was always ready to offer help from anything as small as taking care of culture to sitting through hours of various practice talks. Specific thanks to Anum Azum for being close friend and showing me what a truly devoted scientist looks like. Stephanie Davis López, thank you for being a bench and project partner. For sharing so much of your life and work with me, and for being fairly tolerant of the mess I leave behind my experiments. Thanks to Eddy Kim and Jeff Glasgow for being great senior mentors, and establishing a great culture in a new lab. Thank you Kevin Metcalf, Chris Jakobson, and Mike Ascencio, for broadening the conversation topics of the lab breakroom from science to politics and sports. Special thanks to Mike Fisher for truly framing the scope of small molecule efflux in the lab, and for being the necessary "lab father" to keep us in line.

The entirety of my Ph.D. was framed in a context much larger than the lab. I would like to thank my cohort and friends for being a strong influence outside of the day-to-day research in both work and play. I would particularly like to thank Arunan Skandarajah and Wiktor Stopka. Perhaps it was our slow action to find a place to live that brought us together, but being your roommates was immensely satisfying, and spending the first three years of our Ph.Ds. together made the transition to graduate work that much more bearable. I would also like to thank Phil Guam and Omar Alhashimi for their close friendship. I may have learned more about human nature during our late-night sessions playing Risk than I had in any other class.

I would also like to thank my family. My parents for believing in me, letting me pursue graduate school and always supporting me with everything they could. Even if I had to explain exactly what it is that I did every 6 months, they would always pay attention and try hard to understand. I would also like to thank my brother for encouraging me and reminding me that it was all worth it.

Finally, I would like to thank Stacey Shiigi, the one person that was with me the whole time in graduate school. You were with me through the whole journey, from our first classes to thesis writing. No matter what, I knew that I could seek advice and comfort from you. Without you, I am certain that I would not have been able to complete my work. Unfortunately, I just do not have the words to express the gratitude for everything you have done, so I will just say – thank you.

Chapter 1 - Introduction

1.1 Background

Over the past decade, the biocatalytic production of chemicals has gained increased traction in the scientific community. Organisms provide a large repertoire of enzymes capable of performing unique and specific chemistry in mild reaction conditions. Moreover, a series of reactions can be linked to create a synthetic pathway by expressing multiple enzymes simultaneously in genetically tractable microbial hosts. Synthetic biology has been used to modify all aspects of biocatalaysis, from engineering enzymes with new chemical function[1,2], to controlling reactant flux on the host[3] and pathway[4] scale. Nonetheless, this biochemical production method suffers from the drawback that all reactions must proceed in the cell interior, and all intermediates and final products therefore remain in the reaction pool. This can create problems due to both unintended side-reactions and product inhibition. Thus biocatalysis in vivo has been most successful for producing chemicals of high value, for which high yield is not a consideration, and/or for which the product easily moves out of the cell. The recent focus on microbial production of biofuels[5] and commodity chemicals[6] has considerably altered this paradigm, and subsequently created a need for developing mechanisms of sequestering and removing small molecules from the cell. The utilization of active transporters is a particularly promising strategy for the efflux of biochemicals. Secretion permits the removal of toxic products, allows for lower recovery costs for all products, and can drive reactions forward as products are separated from the rest of the cell.

Small molecule movement in and out of the cell is based on two distinct mechanisms. The first, passive diffusion, is a function of the interaction between the molecule and the lipid bilayer(s) of the cell. For small nonpolar or slightly polar molecules, the diffusion rate is proportional to the product of the partition coefficient of the molecule into an oil phase (the interior of the bilayer) and the diffusion coefficient in that phase[7]. Smaller molecules move faster through the membrane, and more hydrophobic molecules partition more easily. Thus, the majority of bioactive molecules are too large or hydrophilic to easily pass through the membrane. At the same time, many hydrophobic solvents pass through the membrane relatively quickly, which often contributes to their cytotoxicity[8]. To better control the passage of small molecules, cells have a second, active mechanism for moving them across the membrane. Transporters exist for both import and export for most types of molecules including alkanes[9], amines[10], acids[11], esters[12], and many others. Therefore, active transporters provide an engineering platform for designing the transfer of small molecules into and out of the cell.

1.2 Types of efflux transporters

It is estimated that up to 7% of all inner membrane proteins in the model bacteria Escherichia coli are involved in efflux, while more than four times that number are associated with import of small molecules[13]. This disparity highlights the different

approaches the cell takes to controlling the chemical content of the cytosol. While importers are known to be quite specific and often act only on a small class of chemicals or just a single molecule[14,15], exporters have a range of substrate profiles. Some efflux transporters are known to be quite promiscuous[16] in overall activity, while others can maintain high specificity toward their targets[17] . Perhaps the best-characterized class of small molecule exporters in microbes are those responsible for the secretion of antibiotics and other toxic agents, known as multidrug resistance (MDR) pumps[18]. Studies of these transporters have strong relevance for combating increased antibiotic resistance in pathogenic bacteria, but also provide insight into ways that they can be used to modulate the internal chemical environment of the cell. MDR pumps can be classified into several transporter families, grouped by their topology and energy source. For example, Gram-negative bacteria must transport small molecules across two lipid membranes, and use only a single pump to accomplish this action. Pumps in these bacteria utilize one of two primary mechanisms: 1) secreting the small molecule into the periplasm from which transport is accomplished through diffusion across the more porous outer membrane, or 2) employing accessory proteins to channel the substrate through the outer membrane[19]. Most transporters also rely on two distinct mechanisms for obtaining the energy required for transport – hydrolyzing ATP, or using an ion concentration gradient across the membrane. For pumps that use ion gradients, the proton motive force is well-represented as a driving force, yet pumps that utilize Na^+ or K^+ gradients are common as well. For most pumps, one ATP or one ion is required to move one molecule out of the cell. Thus, in systems where production yield of the small molecule is of high importance, ion pumps may be the preferred method for efflux of desired product due to lower total energy cost associated with transport, although other considerations such as total kinetic activity and substrate specificity may favor ATP-based transporters.

1.3 Finding the right transporters

To find the right transporters for secretion of a desired biochemical, two tactics can be taken. The first tactic is a systems biology/transcriptomic approach of discovering transporters which act on the molecule of interest. A genome-wide scan is a particularly fruitful approach for finding native pumps capable of secreting the desired product. This approach requires a screen in which the desired secretion phenotype is linked to growth of the strain such that fractions of populations harboring knockouts or overexpressing relevant pumps will decrease or increase, respectively. To identify candidate efflux pumps, the entire population can be subjected to a transcriptomic analysis. For example, transcriptomic studies of Pseudamonas strains producing p-hydroxybezoate linked the pathway to the production of a toxic intermediate and thus identified overexpression of MDR pumps responsible for p-hydroxybenzoate secretion[20]. These approaches were also used to identify pumps capable of secreting isopentenol in E. coli[21], arenes in Pseudamonas putida[22], and alkanes in Saccharomyces cerevisiae[23]. In addition, mathematical models that take pathway flux into account can help estimate the impact of pumps on the system[24,25]. A

combination of in silico design and transcriptomics was utilized by Lee and coworkers to increase l-threonine production titers in E. coli[26].

The discovery approach works well in hosts where a natural pump already exists. Yet most hosts are chosen for their genetic tractability or ability to produce metabolic pathway precursors, making it difficult to find native pumps capable of secreting the product. Useful transporters may also be found within other organisms such that they must be transferred to the desired host; there are several examples which demonstrate that such heterologously expressed transporters retain their activity in the new context[27–29]. In a seminal study, Dunlop et al. transformed a library of efflux pumps into E. coli and monitored the growth of strains expressing each pump in the presence of toxic concentrations of various biofuels[30]. They identified transporters that increased E. coli tolerance for larger biofuels such as α-pinene and limonine, but not other targets such as short chain alcohols. The inability to find transporters for these alcohols may be due to a small number of putative pumps available, or simply due to the lack of these chemicals in the environment of the cells sampled, because evolutionary pressures had not yet produced suitable transporters. For efflux pumps that do not express well in a heterologous host but are sufficiently homologous to a host pump, protein engineering offers a potential solution. Several studies show that exchanging the substrate-specificity domains between homologous efflux pumps from two different organisms results in altered secretion specificities[31,32].

1.4 Engineering efflux transporters

As biotechnological applications expand, it is becoming necessary to find exporters for molecules not typically found in the environment of common hosts. Known transporters can be engineered through directed evolution methods. Since many exporters secrete multiple substrates, specificity can be altered through relatively few substitutions, especially if structural information on substrate binding sites is available. As with transcriptomic approaches, transporter engineering requires that a phenotype be linked to the action of the pump on the substrate. Demonstrating the utility of this approach, a variety of novel mutants of the E. coli AcrB transporter were engineered for secretion of biofuels over the past several years. AcrB is one of the most studied efflux transporters, with structural[33,34] and kinetic[35] data available for rational design strategies. Competition-based selection was used to identify pumps that secrete biofuels; strains carrying mutagenized AcrB were grown in the presence of exogenously added biofuel at toxic concentrations. In these conditions, strains expressing a pump capable of secreting the biofuel have higher growth rates due to decreased intracellular concentrations of the toxic biofuel, and should dominate the population over time. Follow-up sequencing and phenotype confirmation identifies the mutants.

With this technique, AcrB mutants capable of secreting alkanes[36], olefins[37] , and short-chain alcohols[38] were identified. Interestingly, while secretion of n-octane required mutations to residues lining the substrate binding channel, mutations that gave rise to AcrB activity on short-chain alcohols were not to residues previously identified to be

involved in substrate binding. Instead, the mutated residues were in regions that underwent large conformational changes as part of the efflux process. This indicates that more studies are required to understand the structure-function relationship of these transporters before meaningful rational design approaches can be applied to alter substrate specificity.

1.5 Shortcomings of engineered transporters and future work

The total transporter-mediated flux of a substrate is naturally limited by the number of transporters available. The volume of the membrane is significantly smaller than that of the cytoplasm, meaning that much less total protein can be used for transport. However, increasing the number of membrane transporters is notoriously difficult due to aggregation and toxicity. Overexpression of engineered small molecule transporters was explored by Turner et al. in the context of two different transporters acting in tandem on different substrates[39]. Interestingly, pump expression indeed has an optimum between yielding highest secretion of the molecular product and lowered toxicity from transporter overexpression. Moreover, when multiple transporters are involved, the expression optimum of the combination is different than the optima of the individual transporters. Future research in synthetic biology can address some of these concerns by creating smart genetic networks capable of controlling transporter synthesis as needed – an increase in product concentration would signal for pump overexpression while toxicity of pump production would signal for pump repression.

An additional drawback in engineering transporters is common to most protein engineering applications: since random mutagenesis or transcriptomic studies are the de facto approaches to finding new function, it is crucial to link the secretion phenotype to a growth selection or a similarly high-throughput screening method. While many compounds produced at high titers, such as biofuels, are toxic, the application of efflux transporters should not be limited to only those substrates. Improved strategies for measuring secreted or intracellular concentrations of small molecules will enable advanced engineering of membrane transporters.

Finally, the extracellular membrane need not be the only barrier through which small molecule gradients are established. The ability to sequester pathways and their intermediates inside compartments within the cell can give greater control in balancing reaction rates and avoiding toxic intermediates. Eukaryotes provide a good starting point as their many organelles already perform this function, and the transporters present in the vacuolar or peroxisomal membranes can be repurposed by protein engineering to act on different substrates. In prokaryotes, a similar approach is being sought with control of passive diffusion through bacterial microcompartments, structures similar to the well-known carboxysome[40,41].

1.6 Conclusions

This introduction highlights the developing research into engineering membrane transporters for efflux of small molecules. Secretion of small molecule products from the cell can have vast consequences on overall yield and recovery cost in biocatalysis. Unfortunately, the discovery and engineering of novel small molecule transporters is still a slow process as more tools are required for efficient identification and meaningful rational design of transporter activity and substrate specificity.

In this dissertation we highlight methods for engineering transporters to act on non-native substrates by altering the specificity of the *E. coli* AcrB transporter to accept *n*-butanol as a substrate. We further characterize the activity of the mutant AcrB by building a kinetic model of small molecule transport across the membrane with efflux pumps. We utilize this model to identify transporter expression as a key engineering parameter and develop a genetic system that dynamically regulates expression levels based on membrane toxicity. We further extend the kinetic model to hydrophobic substrates that form an extraneous phase in solution and utilize predictions from that model to find mechanisms for molecular transport of farnesene in yeast.

Chapter 2 - Enhancing tolerance to short-chain alcohols by engineering Escherichia Coli AcrB to secrete the non-native substrate n-butanol.

Reproduced with permission from Fisher, M.A., Boyarskiy, S., Yamada, M.R., Kong, N., Bauer, S. and Tullman-Ercek, D. “Enhancing tolerance to short-chain alcohols by engineering Escherichia Coli AcrB to secrete the non-native substrate n-butanol.” ACS Synthetic Biology, 3, 2014.

2.1 Background

The development of advanced cellulosic biofuels promises to positively impact global climate change, rural development, and energy security.[42-43] Engineered microbes are being used to convert plant biomass into fuels and chemicals.[44-45] However, the toxicity of some of the fuel products to the microbial production host remains a key scientific challenge to the process.[46-47] Biofuel toxicity limits the growth of bacterial and yeast production strains, which in turn limits biofuel titers.[46,48] A number of strategies have been pursued to reduce the toxicity of biofuels to cells, including overexpression of heat shock proteins, modification of the cell membrane, and alteration of the cellular stress response.[49,50] However, it is perhaps most desirable to actively efflux biofuels using membrane transporters, thus reducing toxic effects and potentially improving biofuel recovery.[51-52] Additionally, many fuel-producing reactions in the cell are reversible, and may therefore proceed in either the forward or reverse direction.[53] By pumping the product out of the intracellular milieu, such reversible biofuel production reactions will be pulled in the forward direction, providing an additional increase in productivity. Unfortunately, most biofuel candidates are either not known substrates for microbial transporters,[30] or are not secreted at relevant rates.[54,36]

The RND (resistance-nodulation-division) family of efflux pumps is an attractive starting point for the development of pumps that act on biofuel-like molecules. RND-type efflux pumps are native to Gram-negative bacteria, including *Escherichia coli*, and have a wide range of substrates.[55,56] Moreover, RND-type pumps are powered by the proton gradient rather than ATP and have the potential to secrete compounds directly from the cytoplasm, inner membrane, and periplasm to the extracellular space.[34] As depicted in Figure 2-1A, these pumps are composed of an outer membrane channel (OMP), membrane fusion protein (MFP), and inner membrane pump (IMP).[57] The inner membrane pump has been implicated as the major unit responsible for substrate recognition and extrusion of the compounds.[58,59]

Two recent studies have explored the heterologous expression of transporters in a model organism for bacterial biofuel production, *E. coli*.[30,60] Dunlop et al. screened a panel of 43 RND-type efflux pumps for those that enhanced tolerance to exogenously-added biofuels.[30] They identified transporters that enhanced tolerance to geranyl acetate, geraniol, α-pinene, limonene, and farnesyl hexanoate, and demonstrated that the isolated

efflux pump conferred ~1.5-fold limonene secretion increase in a producing strain. However, none of the 43 transporters enhanced tolerance to *n*-butanol or isopentanol, highly attractive biofuels. Building on this approach, Doshi, Nguyen, and Chang screened 16 ABC (ATP-binding cassette) transporters for those that enhanced secretion of zeaxanthin, canthaxanthin, *β*-carotene, or lycopene from isoprenoid-producing strains.[60] Secretion of these molecules was enhanced ~2.5- to 4.5-fold, again demonstrating the validity of the strategy.

Furthermore, directed evolution has been applied to manipulate the functionality of transporter systems. When an operon conferring resistance to arsenic was evolved by DNA shuffling, it was found that mutations in an inner membrane permease component contributed a 4- to 6-fold increase in arsenite tolerance to *E. coli*.[61] The RND transporter genes have been evolved to increase the tolerance of *E. coli* to antibiotics.[62,63] Very recently, the *E. coli* IMP AcrB was evolved by Foo and Leong to achieve increased secretion of its native substrate *n*-octane.[36] Interestingly, the isolated variants of AcrB in this report also conferred enhanced tolerance to another native AcrB substrate, α-pinene, indicating that the evolution gave rise to a more active pump, but not one with increased specificity to novel substrates.

We show that RND-type pumps can be engineered to act on non-natural substrates and confer greater tolerance to many short-chain alcohols. AcrB from *E. coli* is one of the most well-characterized inner membrane efflux pump proteins from the RND family.[56] In this study we have created libraries of the wild-type AcrB (wtAcrB) efflux pump transporter, expressed these libraries in *E. coli*, and selected AcrB variants that enhance tolerance when cells are grown in the presence of *n*-butanol. Two rounds of directed evolution resulted in AcrB variants that increase log-phase growth by up to 25%. We have

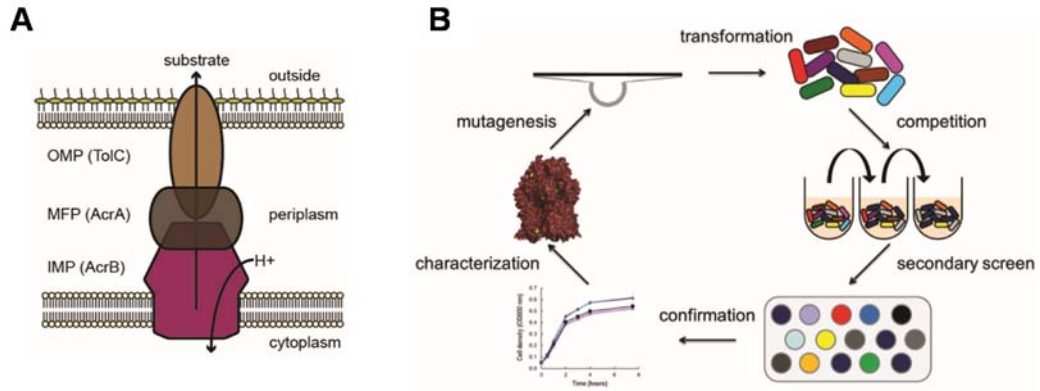

Figure 2-1 Directed evolution to generate tolerance-conferring variants of the AcrB
(A) Schematic of the AcrAB-TolC tripartite pump system. The *E. coli* AcrB protein is an inner membrane efflux pump that works in concert with a membrane fusion protein (AcrA) and outer membrane protein (TolC). AcrB has been implicated in substrate recognition and is a proton antiporter. (B) *E. coli* transformed with libraries of AcrB variants were subjected to exponential growth competition in the presence or absence of 0.5% *n*-butanol. After the competition, cells from both pools were plated, and individual clones were tested for growth performance in *n*-butanol. After confirming AcrB variant-conferred growth, another round of mutation and selection was carried out.

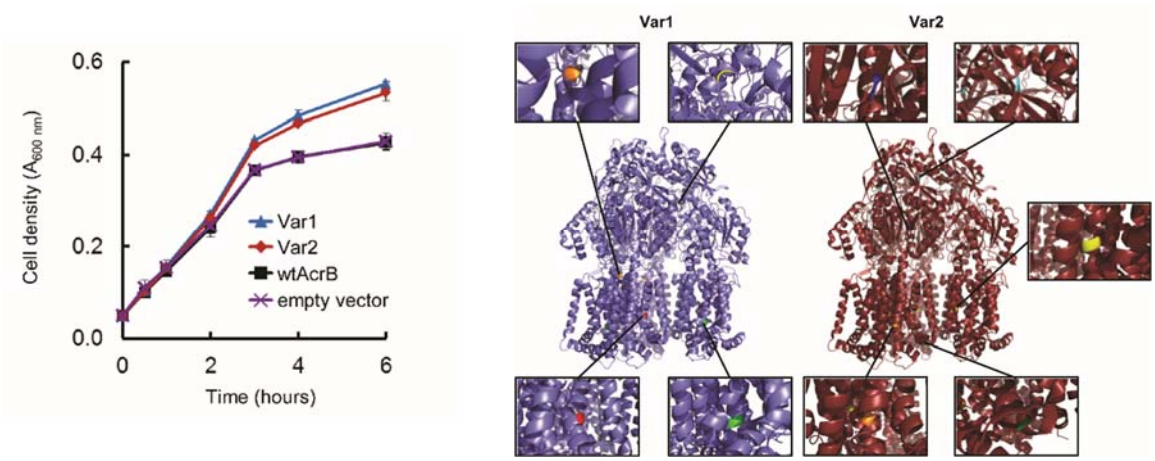

Figure 2-2 AcrB variants Var1 and Var2 confer enhanced growth in the presence of *n*-butanol
Plot of cell growth with respect to time for strains harboring empty vector and wtAcrB controls, Var1, and Var2, in the presence of 0.7% *n*-butanol. Error bars represent one standard deviation of three independent experiments. Right panels show models of AcrB variants. The locations of the mutated residues are noted on a published structure of AcrB. Var1: I370T (red), I466P (orange), G689D (yellow), A942T (green); Var2: E130G (blue), E269G (cyan), M355L (orange), V448A (yellow), T495A (green). PDB entry 2DRD was manipulated using PyMOL.

also shown that these AcrB variants enhance tolerance to a number of short-chain alcohols, but not *n*-octanol, 3-octanol or native AcrB substrates such as ampicillin and chloramphenicol. Individual amino acid changes were found to be responsible for tolerance enhancement conferred by the majority of variants. Importantly, chemical and genetic methods indicate that our AcrB variants actively transport alcohols out of the cell. To our knowledge, this work is the first example in which an RND transporter system has been evolved in the laboratory for the secretion of non-native toxic compounds.

2.2 Results

2.2.1 Generation of initial library of mutagenized acrB

We chose to use a directed evolution strategy (Figure 2-1B) to alter the substrate specificity of the wtAcrB efflux pump from *E. coli*. The entire *acrB* gene was subjected to random mutagenesis and incorporated into a vector under the control of the *araBAD* promoter[64] along with the *acrA* and *tolC* genes, which encode the other two proteins of the tripartite pump. The library comprises 50,000 variants with an average error rate of 0.185%.

2.2.2 Selection via growth competition in n-butanol resulted in enhanced tolerance to alcohols

The *acrB* library was subjected to a selection to identify those library members that conferred enhanced growth in the presence of *n*-butanol. Specifically, *E. coli* cells harboring the library of variants were subjected to an exponential growth competition in the absence (control) or presence (challenged) of 0.5% *n*-butanol. After three rounds of log

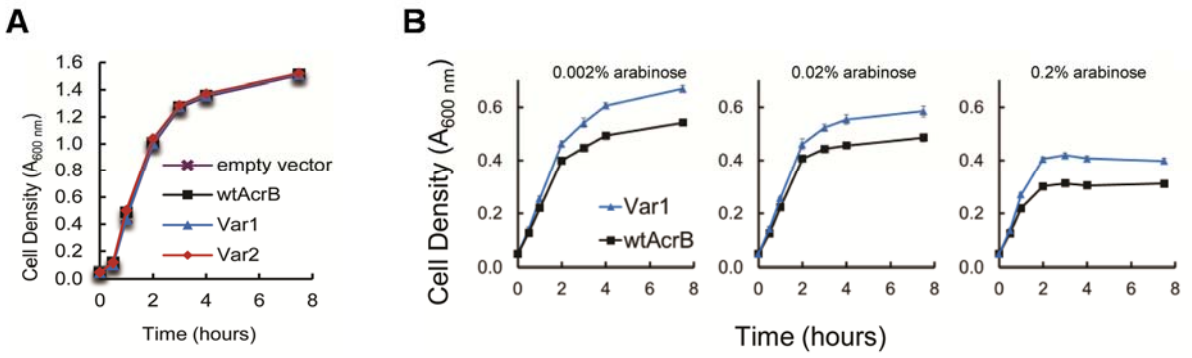

Figure 2-4 Growth of AcrB variants in non-toxic media and under induction conditions
(a) Plot of cell growth with respect to time for the cells harboring wtAcrB, empty vector, or the variant proteins in LB medium with no exogenous addition of any solvent. (b) Increasing wtAcrB and variant pump expression decreases cell growth. Growth curves for strains harboring wtAcrB and Var1 were grown in medium supplemented with 0.7% *n*-butanol and the indicated concentration of inducer. In (a) and (b), error bars represent one standard deviation of three independent experiments.

phase growth followed by serial dilution, dilutions of the remaining cellular populations were plated, and 30 clones from the challenged population and 12 clones from the control population were chosen for further characterization. After back transformation of naïve *E.*

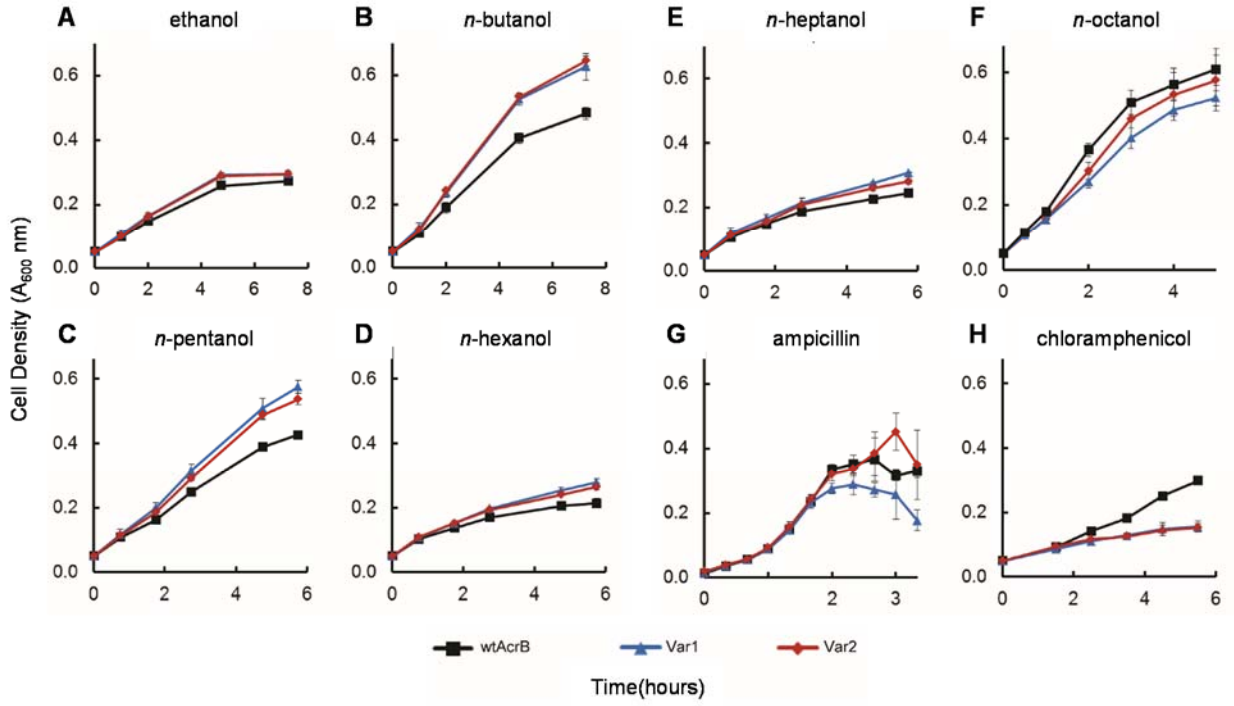

Figure 2-3 Var1 and Var2 confer enhanced growth in the presence of many short-chain alcohols, but not *n*-octanol or antibiotics.
Plots of cell growth with respect to time in medium supplemented with different inhibitors. In 6% ethanol (a), 0.8% isobutanol (b), 0.2% *n*-pentanol (c), 0.1% *n*-hexanol (d), and 0.04% *n*-heptanol (e), Var1- and Var2-expressing strains grow to a greater final cell density than cells expressing AcrB, or harboring empty vector (data not shown). In growth medium supplemented with 0.013% *n*-octanol (f), 20 mg/L ampicillin (g), or 2.1 mg/L chloramphenicol (h), there is no growth advantage conferred by Var1 or Var2. Error bars represent one standard deviation, n=3.

coli DH10B with the plasmids, we carried out growth assays under optimized conditions at 0.7% *n*-butanol. Two positive variants were identified from the challenged population: Var1 (Ile370Thr, Ile466Phe, Gly689AspD, Ala942Thr) and Var2 (Glu130Gly, Glu269Gly, Met355Leu, Val448Ala, Thr495Ala) (Figure 2-2). In the presence of *n*-butanol, these variants conferred growth to higher cell densities (30% and 25% more after six hours of growth for Var1 and Var2, respectively) as compared to cells expressing wtAcrB. All strains grew the same in the absence of inhibitor.(Figure 2-3A) Interestingly, two libraries targeting residues in the periplasmic loop regions of wtAcrB, which have been implicated as substrate-binding determinants,[58,65] did not give rise to any improved variants using the same selection strategy.

We next examined the effect of the two positive variants on growth of *E. coli* in the presence of other toxic small molecules. Compared to wtAcrB and empty vector, Var1 and Var2 also conferred varying levels of enhanced growth, as measured by higher cell densities (and, in some cases, increased log-phase growth rates) to cells grown in the presence of 6% ethanol, 0.8% isobutanol, 0.2% *n*-pentanol, 0.1% *n*-hexanol, and 0.04% *n*-heptanol, but not 0.035% 3-octanol, 2.1 mg/L chloramphenicol, or 20 mg/L ampicillin (Figure 2-4; empty vector data not shown). The variants also did not confer increased tolerance to *n*-octanol at concentrations of 0.005%, 0.012%, or 0.023% after 24 hours (data not shown). Increasing the concentration of inducer reduced the growth of cells harboring both variants and wtAcrB, and did not result in a greater difference in growth between cells expressing Var1, Var2, and the controls in the presence of 0.7% *n*-butanol (Figure 2-3B). Furthermore, as the concentration of *n*-butanol is increased, AcrB variants maintain tolerance enhancement.

2.2.3 A second round of mutagenesis and selection further increased tolerance to n-butanol and isobutanol.

Using the gene encoding Var1 as the parent gene for a second round of whole-gene mutagenesis, we generated a library of 65,000 variants with an average error rate of 0.09%. This second-generation library was subjected to an exponential growth competition in media supplemented with *n*-butanol as well as media supplemented with isobutanol, and a total of 33 clones were tested in the secondary screens. From the isobutanol selection, two more variants, Var1-1 and Var1-2, were identified with improved tolerance over Var1. Notably, compared to wtAcrB, Var1-2 confers a 25% increase in the late log-phase first-order growth rate constant and a 37% higher cell density after six hours for

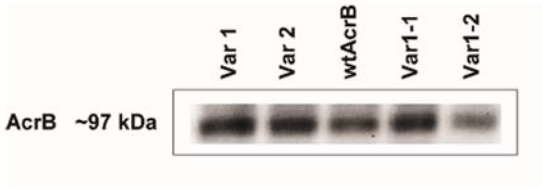

Figure 2-5 Expression of the variants is not significantly different from wtAcrB
A representative anti-His western blot showing the expression levels of the 6xHis tagged AcrB variants after induction with 0.002% (v/v) arabinose. Densitometry performed on three separate blots performed on independent samples revealed no statistically significant variance in expression levels between wtAcrB and any of the variants.

cells grown in *n*-butanol. The additional Var1-1 mutations include Asn144Ser, Ile335Thr, and Ser1043Arg; additional Var1-2 mutations include Asp174Asn, Lys522Gly, and Ser880Pro. It should be noted that none of the mutations significantly altered expression of the variants compared to expression of wild-type AcrB (Figure 2-5).

2.2.4 Butanol concentration within cells is lower for cells expressing Var1-2 than for cells expressing wild type AcrB.

To verify that the growth improvements are due to an increased efflux of *n*-butanol, we set out to determine whether the intracellular level of butanol is altered by the presence of the variants as compared to wtAcrB. To do so, we incubated cells containing either wtAcrB or Var1-2 with 0.6% *n*-butanol and let them equilibrate for one hour. We then measured the amount of *n*-butanol remaining in the buffer and calculated the amount retained by the cells. If the growth phenotype is due to increased *n*-butanol efflux, we would expect to observe higher concentrations of *n*-butanol in the medium incubated with the cells expressing the evolved Var1-2 as compared to wtAcrB, translating into a lower concentration within cells harboring Var1-2. We indeed detected an approximately 15% decrease in *n*-butanol sequestration by the cells expressing Var1-2 over cells expressing wtAcrB (0.552 ± 0.046 μg/ml for Var1-2 versus 0.652 ± 0.020 μg/ml for wtAcrB, $p<0.01$ by two-tailed student's t-test).

It is as-yet unknown how much improvement in tolerance is required for commercial feasibility, as we do not know what amount of *n*-butanol is toxic within the cytoplasm of *E. coli*, nor what concentration will be present in cells producing the *n*-butanol. However, our results indicate that intracellular concentration of *n*-butanol is

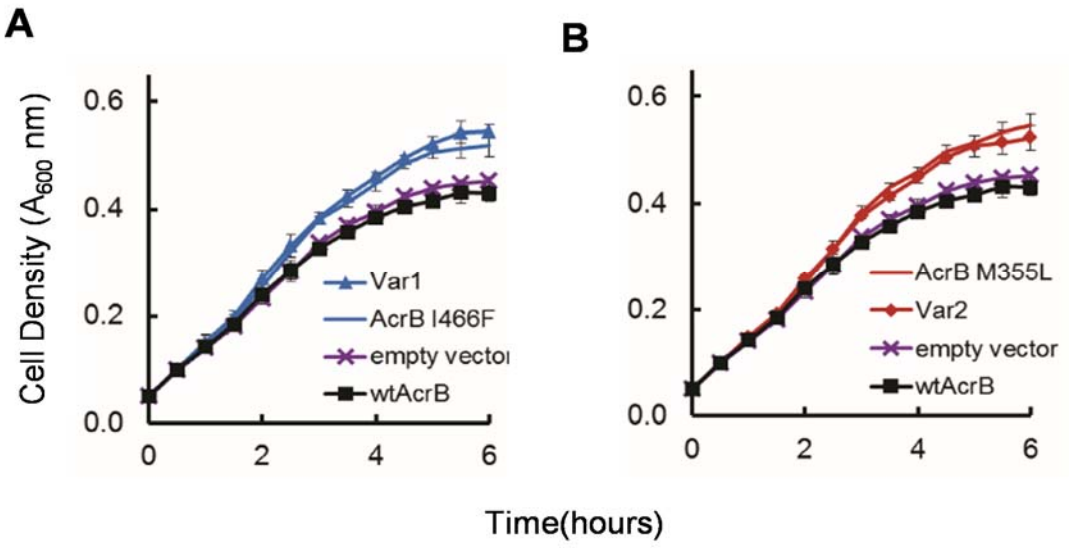

Figure 2-6 Individual mutations are responsible for increased tolerance in butanol in Var1 and Var 2
(A) Growth curves for strains harboring empty vector, wtAcrB, Var1, and AcrB I466F, grown in medium supplemented with 0.7% *n*-butanol. (B) Growth curves for strains harboring empty vector, wtAcrB, Var2, and AcrB M355L, grown in medium supplemented with 0.7% *n*-butanol. Individual mutations in both cases have the same phenotype as the overall mutant. Error bars represent one standard deviation of three independent experiments.

indeed lower in the presence of our top-performing AcrB variant, a result that we expect would be mirrored in butanol-production strains and thus would impact resulting titer.

2.2.5 Individual mutations are responsible for growth enhancement in the presence of n-butanol.

Multiple mutations were observed in all of the variants that enhance growth in the presence of alcohols. To determine which mutations are required for tolerance enhancement, we created each individual mutation found in Var1 and Var2, resulting in nine variants of AcrB mutated at single residues. These sub-variants were then subjected to the *n*-butanol growth assay. It was found that Ile466Phe is wholly responsible for Var1-enhanced growth in *n*-butanol (Figure 2-6A), and Met355Leu is responsible for Var2-enhanced growth (Figure 2-6B). In analogous experiments with the second generation variants, we created each individual mutation from Var1-1 and Var1-2 in the Var1 background. The Var1-2 Ser880Pro mutation was found to be the major contributor to variant-enhanced growth in *n*-butanol (data not shown), while no single Var1-1 mutation was identified to be solely responsible for the tolerance enhancement.

The mechanisms by which mutations in AcrB and homologous pump proteins are proposed to affect transport are difficult to reconcile without experimentally determined crystal structures.[36,63,66]. AcrB is a homotrimer in the assembled pump structure, and rotates through conformations termed “access”, “binding”, and “extrusion” as it effluxes a substrate.[33,67] All three of the contributing mutations identified in our study (Ile466Phe, Met355Leu, and Ser880Pro) are found in transmembrane helices of AcrB, and are in regions of the protein that undergo dramatic conformational changes in the access protomer of the homotrimer.[33,67] Ile466 is at the periplasmic side of transmembrane helix 5 and lines the AcrB central cavity. In the binding and extrusion protomers of PDB entry 2DRD, Ile466 is positioned in the α-helix 1.5 from the helix terminus. However, in the access protomer of 2DRD, Ile466 is modeled as the terminal residue of transmembrane helix 5. The mutation of Ile466 to Phe, a larger and more nonpolar residue, is likely to

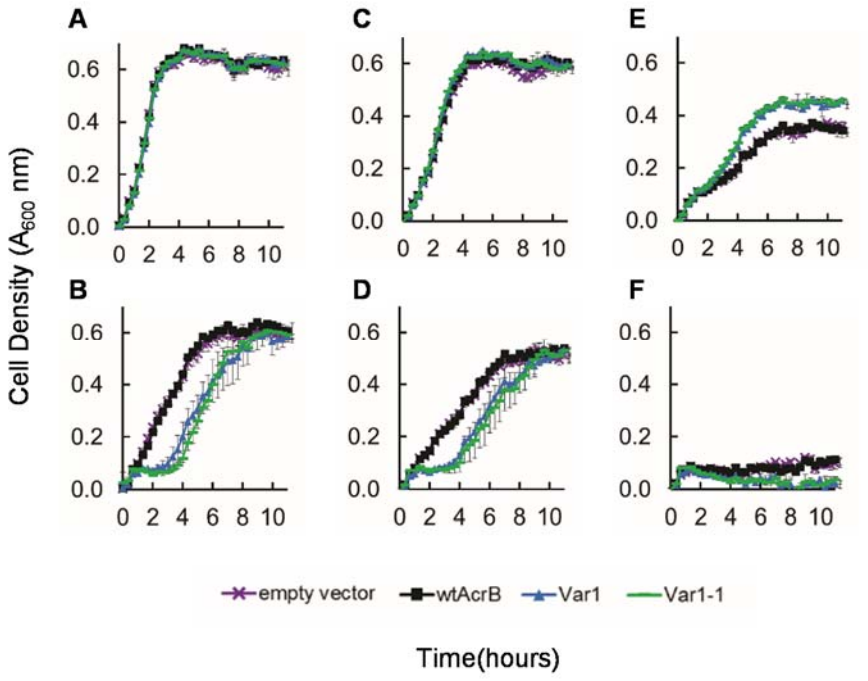

Figure 2-7 Eliminating the proton motive force, eliminates AcrB variant-conferred tolerance
Growth curves for strains harboring empty vector, wtAcrB, Var1, and Var1-1 were grown in medium with 0 (A,B), 0.4 (C,D), or 0.6% (E,F) n-butanol and supplemented with 0.5% glucose, and either with (B, D, F) or without (A, C, E) the proton ionophore carbonyl cyanide 3-chlorophenylhydrazone (CCCP) in microtiter plates. Error bars represent one standard deviation of three independent experiments.

cause an even greater conformational change in the Ile466Phe variant to adjust for steric clashes and water organization if this residue is exposed to the periplasmic environment. As it lines the central cavity, it may also interact with alcohols, contributing to the transport of the compound through AcrB.

Met355 is located on the cytoplasmic side of transmembrane helix 2. In the binding and extrusion protomers, it is half a turn from the terminus. In the access protomer of 2DRD, it is immediately at the terminus. This mutation may disrupt packing and global helix arrangement in the membrane, perhaps even creating enough shift to permit substrate entrance to the central cavity from the cytoplasm. However, when wtAcrB was mutated to contain both Ile466Phe and Met355Leu, the double mutant did not give rise to observable additive or synergistic *n*-butanol tolerance. Thus we conclude that these mutations both result in a broad disruption to multiple transmembrane helices such that it would have been difficult to predict the efflux of butanol using a rational approach.

Ser880 is located within transmembrane helix 8. Transmembrane helix 8 is an interrupted α-helix in the binding protomer, a very long α-helix in the extrusion protomer, and a greatly interrupted α-helix in the access protomer. In the access protomer, Ser880 is only one turn from the periplasmic side helix terminus, compared to two turns away in the binding protomer and five turns away in the extrusion protomer. Proline is a known helix breaker, and so the mutation of Ser880 to Pro likely malforms this helix and perhaps disrupts other transmembrane helices as well, akin to the proposed disruptions brought on by the Ile466Phe and Met355Leu mutations.

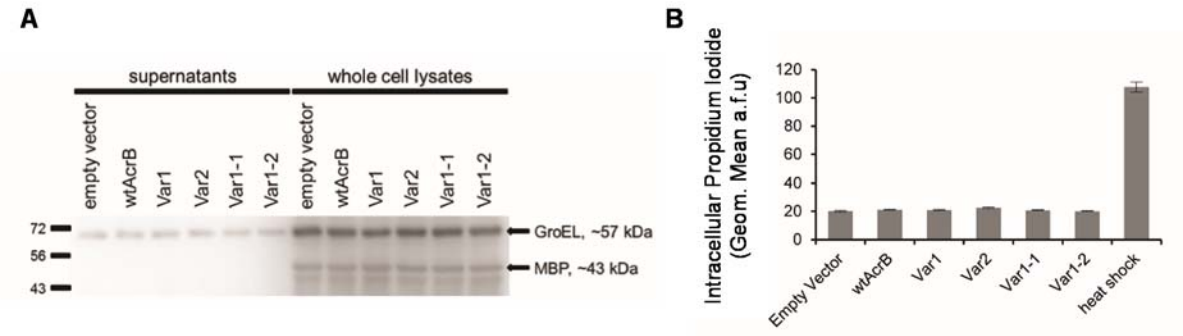

Figure 2-8 The *E. coli* membranes maintain their integrity when AcrAB-TolC are expressed
(A) Western blot analysis of E. coli supernatants and whole cell lysates was performed after the log-phase growth of cells harboring empty vector, wtAcrB, Var1, Var2, Var1-1, and Var1-2. Maltose binding protein (MBP), a periplasmic protein, and GroEL, a cytoplasmic protein, were detected as described in the methods. (B) Permeability of the membrane to small molecules is assessed by propidium iodide staining. Propidium iodide within cells was detected by flow cytometry as described in the methods section for cells harboring empty vector, wtAcrB, Var1, Var2, Var1-1, and Var1-2. A sample of the same strain subjected to heat shock at 80°C for 10 minutes serves as a positive control of membrane damage.

2.2.6 Elimination of the proton motive force disrupts the AcrB variant-conferred tolerance phenotype.

The energy that drives the conformational changes and substrate transport of RND-type efflux pumps is derived from the binding and subsequent release of protons. It is possible to eliminate the proton gradient that exists across the periplasmic membrane, and therefore eliminate the proton motive force, by growing cells in the presence of a proton ionophore.[68] Carbonyl cyanide 3-chlorophenylhydrazone (CCCP) binds protons and carries them through lipid bilayers such as the *E. coli* periplasmic membrane.[69] When our series of strains was grown in the combined presence of *n*-butanol or isobutanol and CCCP, the AcrB variants no longer conferred a growth advantage to the cell (Figure 2-7). In fact, the AcrB variants conferred an extended lag phase which was observed even in growth medium without *n*-butanol or isobutanol. The extended lag phase was followed by log phase growth on par with that of the empty vector and wtAcrB strains, and all strains grew to equal cell densities in stationary phase. This evidence suggests that the activity of the AcrB variants is dependent upon the presence of the proton gradient, and thus that the variants actively transport alcohols out of the cell.

2.2.7 Elimination of the AcrB proton relay functionality disrupts the AcrB variant-conferred tolerance phenotype.

Nikaido and colleagues have identified the wtAcrB residues that are at the wtAcrB proton translocation site; mutating aspartates at amino acid sequence positions 407 and 408 to alanine greatly reduces AcrB activity.[70,71] We made Asp407Ala Asp408Ala double mutant versions of the wild type AcrB and the tolerance-conferring variants. We hypothesized that in the presence of alcohols, the proton relay-deficient variants would no longer confer tolerance. We observe growth that is equivalent to that of cells containing the empty vector or expressing wtAcrB for the various D407A D408A strains. As previously observed, the variants with the intact proton relay residues give rise to a higher cell

density and, for second-generation variants, increased late log-phase growth rates. This indicates that the binding and subsequent release of a proton, and therefore conformational change and active transport, is required to confer tolerance in these strains. Taken together, the experiments with CCCP and the proton-relay mutants support our assertion that the AcrB variants confer enhanced tolerance to *n*-butanol and isobutanol by actively exporting alcohols from the cell.

2.2.8 Low-level overexpression of wtAcrB and AcrB variants does not affect membrane integrity.

Membrane protein expression may affect the integrity of the cell. To rule out any such effects on tolerance, experiments evaluating membrane integrity[72] were carried out. Cells were harvested after log-phase growth, and culture supernatants, 10-fold concentrated culture supernatants, and whole cell lysates were interrogated for the presence of the periplasmic maltose binding protein (MBP) and cytoplasmic chaperone Hsp60 (GroEL). Compared to cells harboring empty vector, none of the cells producing TolC, AcrA, and wtAcrB or AcrB variants exhibit differences in the quantity of MBP and GroEL detected in the supernatants and whole cell lysates (Figure 2-8A). To assess the presence of any smaller membrane perturbations, we also performed staining with the small molecule propidium iodide, which is not a known AcrB substrate. As quantified by flow cytometry, we observe no difference in propidium iodide uptake among cells containing wtAcrB, the variants, or empty vector, while cells damaged by heat shock demonstrate a considerable increase in fluorescence (Figure 2-8B). This shows that the *E. coli* inner and outer membranes are structurally sound with low-level AcrAB-TolC expression, and provides further evidence that the tolerance phenotype we observe is due to the activity of AcrB variants.

2.2.9 AcrB variants do not confer enhanced tolerance in ΔacrB strains

For both *E. coli* MG1655 and BW25113, Δ*acrB* knockout strains grow at a higher rate and to higher final cell densities than the wild-type strains in the presence of the short-chain alcohols *n*-butanol and isobutanol (Figure 2-9). Without these alcohols in the medium, the strains grow at nearly the same rate. Moreover, a recent study using *E. coli* DH1 Δ*acrAB* that screened a panel of 43 naturally occurring efflux pumps, including AcrAB, did not identify any pumps that enhanced *E. coli* tolerance in the presence of the short-chain alcohols *n*-butanol or isopentanol.[30] We therefore suspected that the enhanced growth rate of the Δ*acrB* strains versus the *acrB*$^{+}$ strains in the presence of inhibitory short-chain alcohols would occlude potential growth enhancements conferred by efflux pumps. This was partially confirmed in our experiments in which we expressed our AcrB efflux pump variants in *E. coli* MG1655 Δ*acrB* and observed an enhancement of tolerance compared to wtAcrB expressed from the same vector but not compared to the empty vector control. As expected, we observed growth enhancement for our variants compared to all controls in the *E. coli* MG1655 wild-type background (Figure 2-9), with similar phenotypes as in the *E. coli* DH10B strain in which all our other work was conducted.

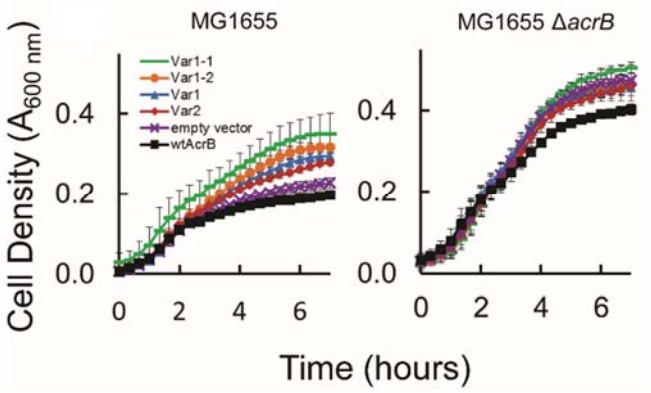

Figure 2-9 AcrB variants do not confer tolerance in *ΔacrB* strains.
AcrB efflux pump variants confer an enhancement of tolerance over wtAcrB and empty vector when expressed in *E. coli* MG1655, but not over empty vector when expressed in MG1655 Δ*acrB*. Growth curves are shown for strains harboring empty vector, wtAcrB, Var1, Var2, Var1-1, and Var1-2 were grown in medium supplemented with 0.7% *n*-butanol in microtiter plates. Error bars represent one standard deviation of three independent experiments.

As described above, our libraries were constructed in *E. coli* strains that retained the wild type *acrB* gene on the chromosome. Since a functional RND efflux pump requires a trimer of AcrB, the presence of wtAcrB permitted the formation of wtAcrB or AcrB variant homotrimers as well as wtAcrB/AcrB variant heterotrimers. However, recent experimental evidence demonstrated that co-expressing AcrB variants is biased in favor of pure trimers versus mixed trimmers.[73] In addition, our expression vectors contain a low to medium copy-number origin (from p15A), and so the resulting expressed protein may be present at significantly higher levels than any background wtAcrB arising from the genome. Thus we suggest that the majority of efflux pumps are likely to be pure homotrimers, be they wtAcrB or AcrB variant, in our system.

2.3 Discussion

With the goals of reducing toxicity, enhancing recovery, and increasing production of microbially-derived chemicals, we have used directed evolution to identify variants of the *E. coli* inner membrane pump protein AcrB that enhance the growth of *E. coli* in the presence of alcohols. Iterative cycles of mutation and selection resulted in the isolation of incrementally improved AcrB variants that enhance the growth of *E. coli* by secreting *n*-butanol and a panel of other straight-chain alcohols. Moving forward, it would be of interest to test these alcohol-secreting pumps in the context of *n*-butanol- and isobutanol-producing strains; the results of such studies will provide further insight into the effectiveness of growth selections using exogenously added compounds at toxic concentrations compared to that of screens in production strains.[48,74] This work provides proof-of-principle that the engineering of transporters for improved tolerance to exogenous inhibitors is effective, and is directly applicable to toxic components of biomass hydrolysates, toxic compounds secreted by another microbe in a co-culture, or compounds that are toxic to a cell in any other constrained environmental context. Importantly, we

have demonstrated that directed evolution of membrane transporters can give rise to specificity for non-native substrates, which will undoubtedly be of use to synthetic biologists as microbes are engineered to produce novel compounds.

2.4 Methods

2.4.1 Strains and bacterial growth condtions.

E. coli Δ*acrB* strains were constructed by P1 transduction and antibiotic resistance cassettes removed from the chromosome according to established procedures[75]. For bacterial growth experiments, Luria Bertani medium/lysogenic broth (LB) was supplemented with 50 μg/mL kanamycin unless otherwise noted. Strains were incubated at 37°C and, when grown in liquid medium, shaken at 225 rpm. When noted, culture densities were monitored at a wavelength of 600 nm (OD_{600}).

2.4.2 Plasmid construction

Plasmids used in this study are listed in Table S2. We constructed a new plasmid, termed pBAD30-Kan, which contains the P_{araBAD} promoter for regulated gene expression, a low-copy origin (p15A, 10-12 copies/cell), and the kanamycin resistance cassette. Briefly, this was done by ligating the gel-purified SphI-AhdI fragment of pBAD18-Kan with the gel-purified AhdI-SphI fragment of pBAD30. Ligation products were used to transform *E. coli* DH10B, and the resulting vector was verified by analytical restriction digestion and DNA sequencing (Quintara Biosciences).

Oligonucleotides used in this study are listed in Table S3. Polymerase chain reaction (PCR) was used to append the restriction sites EcoRI, NotI, and SpeI to the 5' end of the *gfpmut2* gene, and PacI and XbaI to the 3' end of *gfpmut2*. PCR was performed with primers MF1 and MF2 and KOD DNA Polymerase (EMD Chemicals). The resulting PCR fragment and pBAD30-Kan were both digested with EcoRI and XbaI. The digestion products were gel purified and ligated, and the ligation products were used to transform *E. coli* DH10B. The designed insertion site of the resulting vector, pBAD30-Kan-*gfpmut2*, reads NotI(GCGGCCGC)- CTGCAA-SpeI(ACTAGT)-*gfpmut2*-PacI(TTAATTAA)- GCTACT-XbaI(TCTAGA). The vector was verified by analytical restriction digestion and DNA sequencing.

The restriction sites NotI, SpeI, PacI, and XbaI do not occur within the *E. coli tolC*, *acrA*, and *acrB* genes, which code for the AcrAB-TolC efflux pump. PCR was used to generate three DNA fragments from *E. coli* JA300 (gift from Masaaki Wachi) genomic DNA prepared with the Qiagen Generation Column Capture Kit: One each for the *E. coli tolC* (MF3 and MF4), *acrA* (MF5 and MF6), and *acrB* (MF7 and MF8) genes. PCR was performed using KOD Xtreme Hot Start DNA Polymerase (EMD Chemicals). PCR was then used to append a 5' NotI site, a C-terminal 6xHis tag, and a 3' SpeI site to *tolC* (MF9 and MF10), a 5' SpeI site, a C-terminal 6xHis tag, and a 3' PacI site to *acrA* (MF11 and MF12), and a 5' PacI site, a C-terminal 6xHis tag, and a 3' XbaI site to *acrB* (MF13 and MF14). PCR was performed with KOD DNA polymerase (EMD Chemicals). The PCR products encoding either *tolC, acrA, or acrB* were gel purified and digested with NotI and SpeI, SpeI and PacI, and

PacI and XbaI, respectively. The digestion products were purified with the Qiagen PCR Clean Up Kit.

pBAD30-Kan-*gfpmut2* was digested with NotI and SpeI. The vector backbone was gel purified and ligated with the NotI-SpeI *tolC* fragment and the ligation products were used to transform *E. coli* DH10B. The resulting vector, pBAD30-Kan-*tolC-gfpmut2*, was confirmed by analytical restriction digestion. pBAD30-Kan-*tolC-gfpmut2* was digested with SpeI and PacI. The vector backbone was gel purified and ligated with the SpeI-PacI *acrA* fragment and the ligation products were used to transform *E. coli* DH10B. The resulting vector, pBAD30-Kan-*tolC-acrA*, was confirmed by analytical restriction digestion. pBAD30-Kan-*tolC-acrA* was digested with PacI and XbaI. The vector backbone was gel purified and ligated with the PacI-XbaI *acrB* fragment; ligation products were used to transform *E. coli* DH10B. The resulting vector, pBAD30-Kan-*tolC-acrA-acrB*, was confirmed by analytical restriction digestion and DNA sequencing.

2.4.3 Library construction

Whole gene random mutagenesis library: Whole-gene error-prone PCR (0.5 μM MF15 and MF16; 1x GoTaq Green Reaction Buffer; 0.2 mM dATP and dGTP; 1 mM dCTP and dTTP; 5.5 mM $MgCl_2$; and 5 units GoTaq DNA Polymerase (Promega)) was used to generate a pool of mutated *acrB* PCR products. The PCR products were gel purified, digested with PacI and XbaI, purified, and ligated with the likewise digested, gel-purified pBAD30-Kan-*tolC-acrA-acrB* backbone. The ligation products were electroporated into ElectroMAX DH10B-T1^R (Invitrogen) or TransforMax EC100 *E. coli*. After growth for 1.25 hours at 37°C and 225 rpm, cells were spread on LB-agar-Kan plates. Approximately 30,000 colonies were collected in LB-Kan liquid media; these cells were resuspended, and the culture was grown for 1 hour. Frozen stocks of library were prepared in 15% (v/v) glycerol.

CPEC-generated loop 1 library: Error-prone PCR (0.2 mM dATP, dGTP, dCTP, and dTTP; 3 mM $MgCl_2$; 0.4 μM MF17 and MF18; 0.15 mM 8-oxo-2'-deoxyguanosine-5'-triphosphate; 5 μM 2'-deoxy-p-nucleoside-5'-triphosphate; 1x KOD Buffer 1; 1 unit KOD Polymerase; .2 ng/μL template) was used to mutagenize the 567 bp region encoding loop 1 of AcrB. PCR was then used to amplify the mutagenized loop insert fragment (MF19 and MF20) and the vector backbone (MF21 and MF22). Circular polymerase extension cloning (CPEC)[76,77] was used to combine the mutagenized loop insert fragment and vector backbone (0.2 mM dATP, dGTP, dCTP, and dTTP; 1x Xtreme Buffer; 155 ng vector backbone; 12.6 ng mutagenized loop insert; 0.4 units KOD Xtreme Hot Start Polymerase). CPEC products were used to transform ElectroMAX DH10B competent cells (Invitrogen).

Combinatorial site-directed mutagenesis of loop 2 residues: A 72-base oligonucleotide, MF24, was designed with NNK (any base/any base/G or T) codons at amino acid positions 610, 612, 615, and 617 and a 53-base oligonucleotide, MF25, was designed with NNK codons at amino acid positions 626 and 628. DNA polymerase I, large (Klenow) fragment (New England BioLabs) was used to generate double-stranded DNA of this portion of the *acrB* gene. This DNA segment encoded residues 602-635 of AcrB. The DNA segments encoding residues 1-601 (MF15 and MF23) and 636-1049 (MF26 and MF16) were generated by PCR. Overlap PCR was used to assemble the three fragments. The resulting

mutagenized *acrB* was gel-purified, digested with PacI and XbaI, purified, and ligated with the likewise digested, gel-purified pBAD30-Kan-*tolC-acrA-acrB* backbone. Ligation products were used to transform TransforMax EC100 *E. coli* (Epicentre).

2.4.4 Exponential growth competition.

One aliquot of the library was thawed and placed on ice; after mild vortexing, 50 μl was aliquoted into 10 ml LB-Kan medium in a screw-cap test tube (Pyrex No. 9825/6). This culture was shaken for 30 min. The culture was then divided between two screw-cap test tubes. To one of the tubes, *n*-butanol was added to a final concentration of 0.5% (v/v). After one hour of incubation, both cultures were diluted 1:100. Culture densities were monitor until reaching an OD_{600} of 0.4, and then diluted 1:100. Serial dilutions were carried out twice more such that cultures were diluted 1:100 and grown to an OD_{600} of 0.4 a total of three times. Some cells from each culture were then spread onto agar plates.

Single colonies were isolated and used to start overnight cultures. The cultures were diluted to an OD_{600} of 0.05 in liquid medium containing 0.5% *n*-butanol in screw-cap test tubes or microtiter plates.

2.4.5 Characterization of selection output.

For each strain that warranted further characterization and analysis, the plasmid DNA was purified and sent for DNA sequencing. The plasmids were also each used to transform *E. coli* DH10B and spread onto agar plates. Single colonies were used to start overnight cultures. The cultures were diluted to an OD_{600} of 0.05 in medium with the appropriate amount of inhibitor in screw-cap test tubes. Three colonies were analyzed per strain. Culture density was monitored over time with a Genesys 20 spectrophotometer and compared to strains harboring empty vector and wild-type *acrB*. The inhibitors and concentrations used were 6% ethanol, 0.7% *n*-butanol, 0.8% isobutanol, 0.2% *n*-pentanol, 0.1% *n*-hexanol, 0.04% *n*-heptanol, 0.035% 3-octanol, 0.005%, 0.012%, and 0.023% n-octanol, and 2.1 mg/L chloramphenicol. All percentages are given as volume by volume (v/v).

2.4.6 Construction of mutations in *acrB*.

Oligonucleotides (MF28 - MF35) were designed to use the Gibson assembly method for site directed mutagenesis.[78] Whole-vector PCR and Gibson assembly (Gibson Assembly Master Mix, New England BioLabs) was performed as described.

2.4.7 Microtiter plate-based growth assays.

Overnight cultures were diluted to an OD_{600} of 0.05 in 200 μL medium per well containing the indicated concentration of inhibitor. The inhibitor *n*-butanol was used at 0.3%, 0.6%, 0.7%, and 0.8% (v/v), and ampicillin at 20 mg/L. Carbonyl cyanide 3-chlorophenylhydrazone (CCCP) was used at 50 μM and 0.5% (w/v) glucose supplemented to the medium as indicated. Honeycomb microtiter plates (Growth Curves USA) were sealed with MicroAmp optical adhesive film (Applied Biosystems) and incubated in a Bioscreen-C Automated Growth Curve Analysis System (Growth Curves USA) with maximum continuous shaking.

2.4.8 Membrane integrity assays.

Overnight cultures were diluted to an OD_{600} of 0.05 in LB-Kan medium. Cultures were incubated in screw-cap test tubes for 5.5 hours, allowing the strains to complete log phase growth. Samples were normalized by OD_{600}; culture medium supernatants, 10-fold trichloroacetic acid-concentrated culture medium supernatants,[79] and whole cell lysates were assayed for the presence of GroEL and maltose binding protein by western blot.

Western blotting was performed as previously described, but with some changes.[80] Briefly, supernatants, 10-fold concentrated supernatants, and whole cell lysates were mixed with SDS loading buffer containing 2-mercaptoethanol (final concentration loading buffer, 1x). The samples were incubated in a heat block for 5 minutes at 95°C and 10 µL of each sample was run on 12.5% Tris-glycine gels. Proteins were transferred to a polyvinylidine fluoride membrane (Immobilon-P, Millipore) using the Trans-Blot SD Semi-Dry Transfer Cell (Bio-Rad). The membranes were blocked in 5% (w/v) nonfat dry milk/TBST buffer (20 mM Tris-HCl, 150 mM NaCl, 0.05% Tween-20, to pH 7.5) at room temperature for 1 hour. The membranes were incubated with primary antibodies diluted in 1% milk/TBST at room temperature overnight. The following primary antibodies were used: monoclonal mouse anti-maltose binding protein (Sigma), diluted 1:5000, and polyclonal rabbit anti-GroEL (Sigma), diluted 1:10000.

After washing in TBST, the membranes were incubated with secondary antibodies diluted in 1% milk/TBST at room temperature for 1 hour. The following secondary antibodies were used: Stabilized Peroxidase Conjugated Goat Anti-Mouse, H+L (Thermo Scientific), diluted 1:1000, and Stabilized Peroxidase Conjugated Goat Anti-Rabbit, H+L (Thermo Scientific), also diluted 1:1000. After washing, proteins were detected using the SuperSignal West Pico Chemiluminescent Substrate (Thermo Scientific) and images captured with a ChemiDoc XRS+ imaging system (Bio-Rad).

Chapter 3 - Kinetic model of efflux transporters in microbial production strains

3.1 Background

Efforts to engineer efflux pumps for the secretion of small molecules out of the cell are, to date, almost entirely empirical. Techniques are established to identify pumps with desired specificities through screening libraries of homologues from different species[30] and to generate pumps with new activities via random mutagenesis[36,38]. More predictive approaches are needed, however, to increase the collection of pumps capable of specifically secreting a diverse set of molecules at levels relevant to biotechnology. Structure-function relationship studies can help identify which residues need to be mutated within the transporters to confer changes in specificity or increased function. Meanwhile, mathematical models for the kinetics of transport can aid in selecting pumps with activities that best match production needs. In addition, a quantitative understanding of the mechanisms and capacity of secretion enables the identification of the most critical parameters to engineer membrane transporters. For example, quantitative predictions into relative strengths of diffusion and efflux for various solvents can guide researchers as to whether strain engineering of membrane composition or protein engineering of transporters is the more promising approach for increased tolerance and titer. This insight is especially important in the engineering of membrane transporters as their activity is tied with toxicity[81]; thus, optimization of function is crucial in engineering efforts.

Natural small-molecule efflux systems are known to act on a variety of compounds toxic to the cell. The systems of enterobacteria have been studied more extensively for their medical significance. Pumps such as the AcrA-AcrB-TolC system respond to a wide variety of toxic compounds including bile salts and antibiotics. Although the capability of AcrB to secrete antibiotics reduces antibiotic effectiveness, antibiotic resistance often requires other proteins to inhibit activity of the antibiotic. The likely reason is that efflux pumps are only able to secrete their targets up to a maximal rate. Pumps cannot maintain sub-inhibitory concentrations inside the cell as extracellular concentrations become high[82]. Typically, antibiotics are inhibitory in the μM concentration range, yet production of commodity chemicals and biofuels, such as *n*-butanol often reaches titers greater than 1 mM extracellularly[83]. This disparity indicates that efforts to employ pumps effectively for biochemical production require 1) a deeper understanding of both the kinetic thresholds of efflux transporters and 2) identification of the properties that will maximally increase yields upon optimization.

We demonstrated previously (Figure 2-5) that the mutants of AcrB act on a variety of primary alcohol substrates, but the increase in tolerance diminishes with increased molecular weight of the alcohol. One possible reason for this behavior is that longer-chain alcohols are unable to be accommodated in the substrate binding cavity of the mutated AcrB[59]. This hypothesis is unlikely, because AcrB is known to act on multiple substrates

that are significantly larger than the largest alcohols used in the tolerance study[34]. If we assume that AcrB acts at approximately the same rate on all of the alcohols, then the tolerance of the strains expressing the alcohol-secreting variants of AcrB should be greater for longer alcohols as they are toxic at lower exogenous concentrations. Thus, even the smallest amount of efflux should be very beneficial. The observed reduction in tolerance with increasing chain length indicates that additional factors affecting the transport of small molecules across the membrane must be considered.

To this end, we have pursued the creation of a kinetic model that includes diffusion and active transport kinetics of small, polar, non-ionic molecules across the membrane. We can extend this model to include industrially relevant butanol production dynamics to investigate critical parameters for transport. Further, quantitative understanding of the transport process can aid in future design of transporters and in finding likely substrate candidates for successful transport.

3.2 Model Formulation

The model is divided into two compartments: intracellular and broth. The cell is treated as a compartment with complete mixing. Transport of small molecules occurs through a single interfacial boundary based on the well-known permeability of the *E. coli* outer membrane to small molecules[84]. Accumulation of the small molecule in each of these compartments is then given by the following equations

$$V_c \frac{dC_c}{dt} = V_c r_m - A_c(J_{ac} + J_{diff}) \qquad \text{Cell} \qquad (3\text{-}1)$$

$$V_b \frac{dC_b}{dt} = A_c(J_{ac} + J_{diff}) \qquad \text{Broth} \qquad (3\text{-}2)$$

Where V and C are the volume and concentration of the product, respectively, in each compartment ($_c$=intracellular, $_b$=broth), A is the area of the interface between two compartments, and r_m is the molecular production rate of the butanol. J_{ac} and J_{diff} are the active and diffusive fluxes of butanol across the membrane, respectively (mass butanol per unit area per second). We assume a constant volume of the broth and cells to mimic culture conditions where biomass is first grown to production volumes and then all energy is expended into butanol production rather than growth. In the current formulation, we keep a constant production rate even though most production systems decrease in production over time due to cell death or product inhibition.

Diffusion of polar, hydrophobic molecules across the lipid membrane has been well studied and depends on the oil/water partition coefficient $K_{oil/water}$ and the diffusivity of the molecule in the lipid environment of the lipid membrane (Marrink 1996). The flux across the membrane is given by Equation 3-3 below.

$$J_{diff} = \frac{KD}{\delta}(C_c - C_b) \qquad (3\text{-}3)$$

Where K is the partition coefficient (~10^{-6}), D is the diffusivity of the compound in an oil phase (~10^{-6} cm^2/s) and δ is the length of the hydrophobic region of the lipid bilayer (~3 nm). Diffusion is passive and depends on the concentration gradient between the cell and the broth. The overall transmissibility, $\frac{KD}{\delta}$, for butanol has been calculated and empirically measured to be near 1 μm/s[85].

To model active molecular transport across the cell membrane, we utilized kinetics studies performed on the transport function of AcrB. In particular, the dynamics of AcrB function are characterized for native beta-lactam substrates[35,86]. The best fit expression for the kinetics of the AcrB transporter is the modified Hill equation[35]:

$$J_{ac} = \Gamma_t \nu_{max} \left(\frac{{C_c}^n}{K_m + {C_c}^n} \right) \tag{3-4}$$

Where Γ_t is the number of transporters per unit cell area, ν_{max} is the maximum efflux rate, $K_m$is the concentration of substrate required for the rate to be half of ν_{max}, and n is the Hill coefficient. Experiments on the native substrates of AcrB revealed that $n = 2.7 - 3.1$ and $K_m = 0.1$ μM for a variety of beta-lactams. This value of K_m is significantly lower than the concentration of molecular butanol in solution of a production strain[87], reducing the flux expression in those cases to $J_{ac} = \Gamma_t \nu_{max}$.

While the production rate for each system highly depends on the metabolic pathways and fermentation conditions of the host cell. Nevertheless, key features of the model can be glimpsed from examining the steady-state case. In our system using the butanol-secreting AcrB variant, *n*-butanol was not produced during the growth assays. Instead, the metric for enhanced butanol efflux was the relative decrease in toxicity of *n*-butanol inside the cell. Since cytotoxicity is generally associated with the expiration of small molecule production, we can model the production rate as decreasing with relative toxicity.

$$r_m = r_{m0} \left(1 - \left(\frac{C_c}{C_{tox}} \right)^p \right) \tag{3-5}$$

Here r_{m0} represents the maximal production rate when the cell is not perturbed by product toxicity, while C_{tox} is the concentration of the product that is maximally inhibits all production. The coefficient p is empirically determined and is likely to be unique for each production strain.

3.3 Results

3.3.1 Mathematical model predicts reduced benefits from AcrB variants on longer-chain alcohols at steady-state.

We first tested the validity of the model by applying the parameters used in our toxicity studies to the model. In our experiments, we noted that the tolerance afforded by the mutated variants of AcrB decreased as the molecular weight of the alcohols increased.

In our experiments, the cells did not produce any of the alcohol ($r_m = 0$) and cells were grown into stationary phase, where steady-state can be assumed. In addition, since the alcohol is added exogenously, diffusive transport is occurring from the broth to the cell. Combining equations 3-2 through 3-4 with these assumptions, we probe the potential benefit of the pumps by expressing the concentration gradient achieved through alcohol secretion.

$$\Delta C = (C_b - C_c) = \frac{\Gamma_t \nu_{max} \delta}{KD} \qquad \begin{matrix}\text{Steady-state} \\ \text{exogenous alcohol}\end{matrix} \qquad (3\text{-}6)$$

Our studies were performed at alcohol levels close to the toxicity limit ($C_b = C_{tox}$). Within this limit, cells that have no pumps capable of secreting the alcohol ($\nu_{max} = 0$) will be in a solution where the extracellular and intracellular concentrations remain the same ($C_b = C_c = C_{tox}$) as determined from the steady-state achieved through diffusion. However, cells that express active pumps will achieve an extracellular environment enriched in the alcohol, lowering the intracellular concentration. This benefit can be normalized to the toxicity concentration for a particular alcohol and expressed as follows from equation 3-6 and $C_b = C_{tox}$.

$$\frac{C_c}{C_{tox}} = 1 - \frac{\Gamma_t \nu_{max} \delta}{KDC_{tox}} \qquad (3\text{-}7)$$

Since alcohol toxicity is dose dependent, the lower the ratio of the cellular concentration of the alcohol to the toxic concentration, the higher the growth rate. At first glance, it would seem that the benefits of the pumps would be increased for higher molecular weight alcohols. C_4-C_{10} alcohol toxicity is roughly proportional to the molecular weight of the alcohol, such that each carbon reduces C_{tox} by two-fold[55]. This reduction would manifest in decrease of the ratio of cellular concentration to the toxic concentration, thereby increasing the benefits of having an efflux pump that is able to recognize the alcohol. However, two other parameters are changed by the increase in molecular weight of the alcohol. The diffusivity of the alcohol across the membrane is decreased, although almost negligibly, and the partition coefficient of the alcohol into the oily membrane is increased. This change in partition coefficient has been characterized and is remarkably close to 10-fold for each additional carbon after C_4[88]. This makes the product of KDC_{tox} increase by about 5-fold for every additional carbon, thereby reducing the overall positive effect of the pumps on alcohol tolerance. This finding is consistent with the growth data we obtained for various AcrB variants in C_4-C_8 primary alcohols.

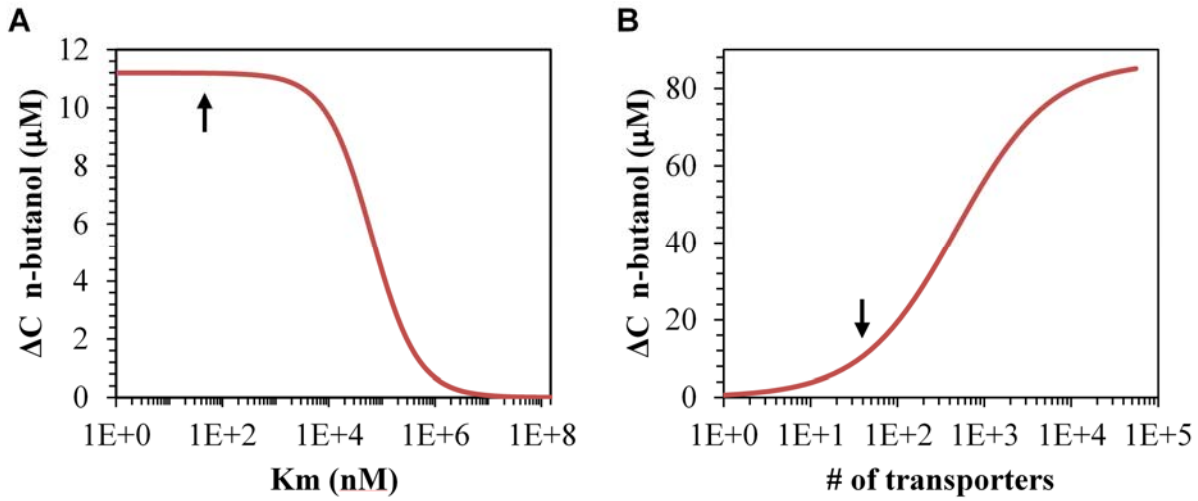

Figure 3-1 Predicted *n*-butanol concentration gradient as a function of transport parameters. Plots indicate difference in *n*-butanol concentration between the inside and outside of the cell after modeled production as a function of changing K_m (A) or Γ_t (B). Arrows show values for wild-type AcrB transporters in E. coli acting on native substrates. A 72 hour production cycle was modeled with 87μM *n*-butanol concentration considered inhibitory to production.

3.3.2 Transporter expression is an important engineering consideration

We next extended the cell transport model to a system in which *n*-butanol is produced intracellularly until toxicity of the butanol stops production. In our calculations, we used a toxic concentration of *n*-butanol of 87 μM, based on previously performed toxicity studies. We simulated the production of butanol for 72 hours following an initial production rate consistent with already existing pathways. We monitored the concentration gradient of *n*-butanol inside and outside of the cells as we varied possible engineering parameters. The two main parameters that can be engineered are substrate specificity, K_m, and the number of membrane transporters per cell, Γ_t. Figure 3-1 shows the change in the concentration gradient at the end of the production run as a function of these parameters. Interestingly, the substrate specificity does not play as large a role in the potential efflux the *n*-butanol out of the cell. Km values 2-3 orders of magnitude higher than those of known substrates for AcrB yield roughly the same concentration gradient. The expression of the transporter protein, however, shows a large possible increase the concentration gradient, and subsequently in titer, of butanol. Since AcrB expression levels are fairly low, and are known to increase substantially when induced, our model indicates that after initial screening for transporters that can act on a substrate, future engineering efforts may best be placed into the increase of transporter numbers in the cell. This is further confirmed in findings of increased *n*-butanol tolerance and production through engineered pump expression (see Chapter 4).

3.4 Discussion

The kinetic model framework described above can be a useful tool for predicting the behavior of engineered pumps with regards to their substrates. Using this model, we

were able to identify key features of the system that resulted in differing tolerance levels of engineered AcrB variants to primary alcohols. We show that pumps have a greater impact on the secretion of larger, less hydrophobic molecules due to their decreased membrane permeativity. For small molecule production at high titers, the relative substrate specificity exhibited by the somewhat promiscuous pumps such as AcrB is sufficient for maximum benefit. In these cases, engineering of the transporters does not depend on finding mutations that increase pump-substrate interactions significantly, but rather relies on finding pump variants that are capable of recognizing the substrate to some degree and are able to increase overall reaction rate of the pump or allow for higher transporter expression levels within the cell. Pump overexpression has been shown to be toxic to their native hosts, and therefore requires further engineering controls to maximize expression while minimizing supplementary toxicity.

Chapter 4 - Dynamic Regulation of Efflux Protein Expression for Increased Tolerance to and Production of *n*-butanol.

4.1 Introduction

Microbial production of small molecules at high titer is often hindered by the toxicity of the product to the host organism. While multiple approaches exist to alleviate this toxicity through strain engineering, one of the most promising strategies is the use of efflux pumps to secrete the molecules out of the cell [89,90]. This tactic has the benefit of relieving product toxicity with minimal alteration to the host cell, while also providing a way to increase titers through removal of product inhibition and potentially aiding in product separation from biomass. Indeed, efflux pumps have been used or engineered for the removal of multiple biofuel molecules including alkanes [54], olefins [37], alcohols [91,92], fatty acids [12], and terpenes [30].

In *E. coli*, the multidrug efflux pump AcrB-AcrA-TolC natively effluxes antibiotics, surfactants, and hydrophobic solvents [93,94]. The inner membrane pump component, AcrB, was successfully targeted by multiple engineering efforts to secrete industrially important chemicals [37,92,95], including the next-generation biofuel *n*-butanol [38]. Butanol is known to be toxic to the cell putatively through interactions with the cell membranes [96,97]. Evolved variants of the AcrB transporter were able to alleviate some of this toxicity through *n*-butanol secretion.

As is the case for many membrane proteins, however, the overexpression of efflux pumps often inhibits cell growth. Thus, in a biochemical production context, optimal expression is required to balance the toxicity associated with the overexpression of these membrane proteins with the advantages they provide. The expression profiles that achieve this result depend not only on the pumps themselves, but also the host strains, and even the various combinations in which the pumps are used [39]. Ideally, the cell would be able to sense the membrane environment and respond accordingly to express the efflux pumps at a maximal, nontoxic level in an inducer-independent context. The latter constraint would reduce the use of expensive small molecules on the industrial scale.

Genetic circuits offer a solution to these challenges. To design a system that is able to control membrane transporter levels, the circuit must respond to membrane protein overexpression stress while ignoring cell envelope stress from the product itself. Recently, dynamic regulation systems to control metabolic pathway enzyme expression have been engineered to sense metabolite concentration [98], and detect the toxic build-up of intermediates [99]. Thus far, these systems have been designed to respond to either specific metabolites or to general cellular stress, rather than to a specific type of stress. Nonetheless, the concept holds promise for the regulation of membrane transporter levels.

Here we utilize the native promoter of the gluconate metabolism operon, $P_{gntK,}$ to sense membrane stress specific to transporter overexpression. Placing *acrB* under the control of this promoter is sufficient to create a negative-feedback loop that dynamically controls AcrB expression to minimize cellular toxicity. Strains in which P_{gntK} controls the expression of a butanol-secreting mutant, AcrBv2, are as tolerant to *n*-butanol as strains

for which AcrBv2 expression was optimized. Strikingly, these strains are also capable of producing up to 40% more *n*-butanol when co-expressing *n*-butanol production pathways. This dynamic regulation extends to other membrane-associated *E. coli* proteins and thus will be broadly useful in quickly finding ideal, non-toxic expression levels for membrane proteins for a range of applications.

4.2 Results

4.2.1 Identification of a responsive promoter to AcrB toxicity

To create a negative feedback loop capable of responding to AcrB-induced membrane stress, we first needed to identify a promoter that is negatively regulated specifically in response to this type of stress. To find such a regulator, we assembled a set of promising promoters known to respond to cell envelope stress signals as reported by Moen et al [100]. We selected the promoter regions upstream of genes that had a two-fold or higher change in expression in response to stress and only responded to one or two classes of envelope stress, in order to avoid promoters that are part of a general stress response. Many of the promoters are not yet well-characterized, thus we chose regions from 500 bases upstream to the start of these genes (or operons where appropriate) to represent the putative promoters of these systems. We then cloned the library of putative promoters upstream of the gene encoding a red fluorescent protein (RFP) in *E. coli* DH10-B cells. In the same strains we placed *acrB* on a second plasmid under the control of an arabinose-inducible P_{bad} promoter, and subjected cells to stress from increased AcrB expression by

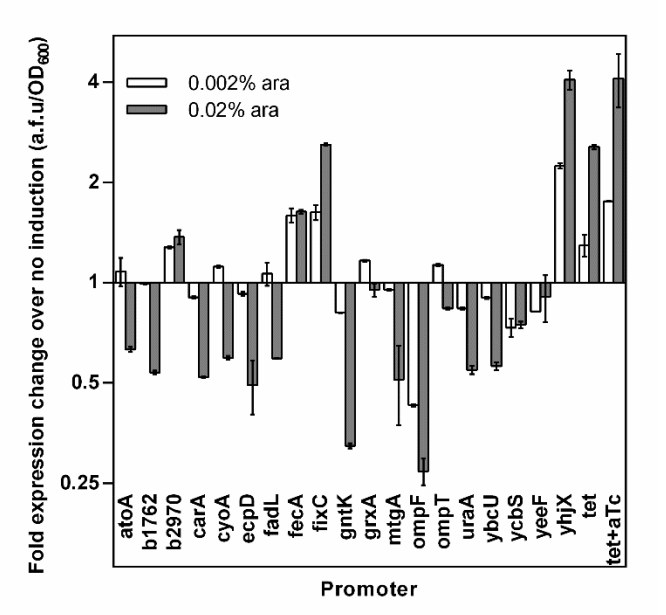

Figure 4-1: Stress promoter response to AcrB overexpression.
Putative stress promoters were cloned upstream of mcherry (RFP) and transformed into strains containing the Pbad-acrB vector. Expression is shown as relative change in RFP fluorescence compared to no inducer added after normalization to the number of cells (OD600). Tet and tet+atc are control vectors containing the Ptet promoter without and with addition of the aTc inducer (100ng/mL) respectively. Error bars denote one standard deviation, n=3.

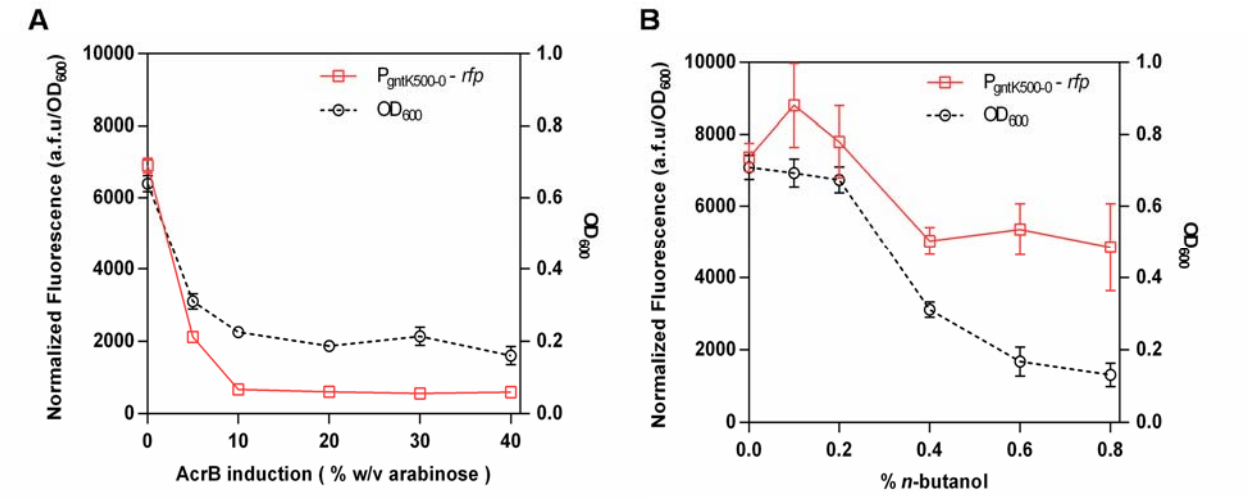

Figure 4-2: PgntK response to envelope stress.
Fluorescence as a function of toxicity from the PgntK500-0-mcherry vector in response to Pbad-acrB overexpression (A) or addition of exogenous n-butanol (B) and the corresponding measurement of toxicity OD600. Cell fluorescence and OD was measured 6 hr after induction or addition of n-butanol. While PgntK500-0 does respond to n-butanol, the response is more tempered and occurs at higher toxicities than the response to AcrB overexpression. Error bars show one standard deviation, n=4.

titrating in arabinose in several cultures. The promoters responded in a variety of ways to this stress (Figure 4-1 includes representative members of the library). Of the promoters not involved in overall cell stress, the putative promoter region from the *gntK* operon ($P_{gntK500\text{-}0}$) conferred the highest decrease in RFP expression. The tetracycline-inducible P_{tet} promoter, in both the induced and uninduced states, served as a control for general expression response to AcrB.

4.2.2 P_{gntK} is inhibited by AcrB overexpression but not *n*-butanol toxicity

We extended the use of our RFP reporter system to measure the response of $P_{gntK500\text{-}0}$ to varying stress levels. We assessed the expression of RFP from the promoter as a function of AcrB overexpression by monitoring AcrB levels with an AcrB-GFP fusion protein. The expression of this fusion was under the control of a P_{bad} promoter from a second, high-copy (colE1 origin of replication) plasmid. We analyzed RFP and GFP fluorescence in strains with varying arabinose induction levels. $P_{gntK500\text{-}0}$ has a uniformly negative response to acrB overexpression stress until it is fully repressed down to the basal level (Figure 4-2A). After full repression, additional increase in AcrB expression has no effect on the promoter. A similar experiment was performed with the addition of *n*-butanol as the stress inducer, as it is important in our scheme that the negative feedback response is limited to the stress associated with AcrB overexpression and not the toxicity from *n*-butanol (Figure 4-2B). While there is some decrease in promoter activity due to *n*-butanol toxicity (~33% decrease), this response is not as severe as the one generated by AcrB overexpression (12-fold decrease).

4.2.3 P_{gntK} responds to AcrB overexpression through a unique repression mechanism

The regulation of the *gntK* promoter has been previously studied by Izu et. al [101]. P_{gntK} controls the expression of the gluconate kinase (GntK) with read-through to the gluconate importer (GntU). The promoter region was shown to begin at -169bp from the start of *gntK*, and indeed, when we made a truncation to the putative promoter to include only 200bp upstream of the start site rather than 500, the response to AcrB overexpression was the same. The region from -100bp resulted in almost no constitutive expression and did not respond to AcrB overexpression (Figure 4-3A). In this study we will refer to the 200-0bp region upstream of *gntK* start site as P_{gntK}. The promoter is catabolically repressed [102] and is acted on by a repressor (GntR) which is constitutively expressed upstream of the *gntK/U* operon. In addition, evidence also suggests that GntK itself inhibits P_{gntK}, although the levels of inhibition are significantly lower than that from GntR. We investigated whether the P_{gntK} response to AcrB overexpression was mediated by GntR or GntK. To this end, we used knockout strains of BW25113 *E. coli* from the Keio knockout collection[103] with *gntR* and *gntK* excised from the genome. Figure 4-3B shows the response of P_{gntK} to AcrB overexpression in these strains normalized to the response in wild-type *E. coli* without AcrB overexpression. As expected, RFP production from P_{gntK} was somewhat increased in Δ*gntK* strains and even more so in Δ*gntR* strains. Deletion of *gntK* or *gntR* did not interfere with AcrB induced repression of $P_{gntK,}$ indicating that this repression mechanism was separate from the known repression by GntR or GntK. Furthermore, due to increased expression in the knockout strains without AcrB induction, the repression from AcrB overexpression was increased in the knockout strains.

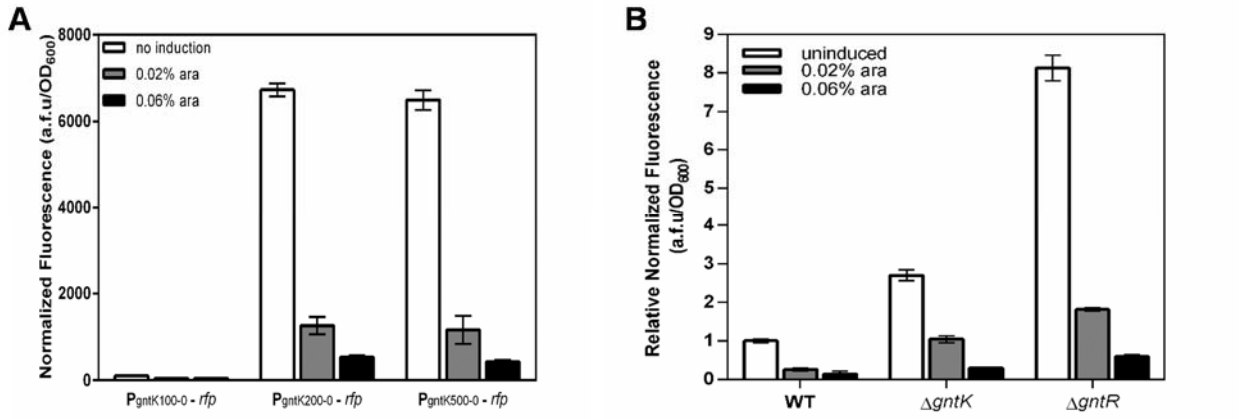

Figure 4-3: PgntK truncation activity and response to AcrB overexpression.
(A) Cells containing the plasmids with AcrB under the control of the inducible Pbad promoter were transformed with plasmids containing PgntK truncations driving RFP expression. Promoter activity was then monitored by RFP fluorescence 6 hours after induction. The 500-0 and 200-0 promoter truncations behave identically while the 100-0 truncation loses all promoter activity. (B) ΔgntK and ΔgntR strains show an overall increase in expression, but the repressive response to AcrB overexpression is still present. Wild-type, ΔgntK, and ΔgntR strains of E. coli BW25113 were transformed with Pbad-acrB and PgntK-rfp containing plasmids and RFP expression was monitored in response to AcrB overexpression. All levels were normalized to expression from the wild-type strain with no acrB induction.Error bars show one standard deviation, n=3.

4.2.4 P_{gntK} responds to overexpression stress from other membrane proteins

To evaluate how specific the response of P_{gntK} is to AcrB overexpression, we monitored the activity of the promoter in response to overexpression of other proteins. We placed various membrane and cytoplasmic proteins under the control of P_{tet} promoter as translational fusions to GFP. We then co-transformed cells carrying these plasmids with the P_{gntK}-*mcherry* plasmid to monitor P_{gntK} response. Overexpression of FepC, a cytoplasmically-associated inner membrane protein involved in transport of enterobactin [104] (Figure 4-4A), AmpC, the periplasmic beta-lactamase [105] (Figure 4-4B), and FucP, a fucose transporter [13] (Figure 4-4D) produced the same response of repression in P_{gntK} relative to toxicity level. However, overexpression of two non-toxic proteins, cytoplasmic GFP (Figure 4-4F) or membrane-localized ATP synthase subunit AtpF (Figure 4-4E), did not induce a decreased expression profile from P_{gntK}. Similarly, the toxic overexpression of the cytoplasmic protein GroEL [106] did not elicit a strong response from P_{gntK}, even though cell growth was impaired (Figure 4-4C).

4.2.5 P_{gntK} maintains AcrB levels through negative-feedback

To confirm that AcrB expression could be controlled by P_{gntK}, we placed an a*crB:mcherry* fusion with the native AcrB ribosome binding site under the control of P_{gntK}. We again overexpressed AcrB-GFP via an inducible promoter and monitored AcrB-RFP expression in wild-type BW25113 and Δ*gntK E. coli* strains. P_{gntK} maintains the same repression phenotype when controlling AcrB expression as it does when controlling the RFP reporter alone. Interestingly, the response in the Δ*gntK* strain was stronger, with a greater constitutive expression level as well as a stronger response to AcrB-GFP overexpression (Figure 4-5A). We confirmed the inverse relation between overexpressed AcrB-GFP and P_{gntK}-controlled AcrB-RFP in the Δ*gntK* strain by western blot analysis (Figure 4-5B).

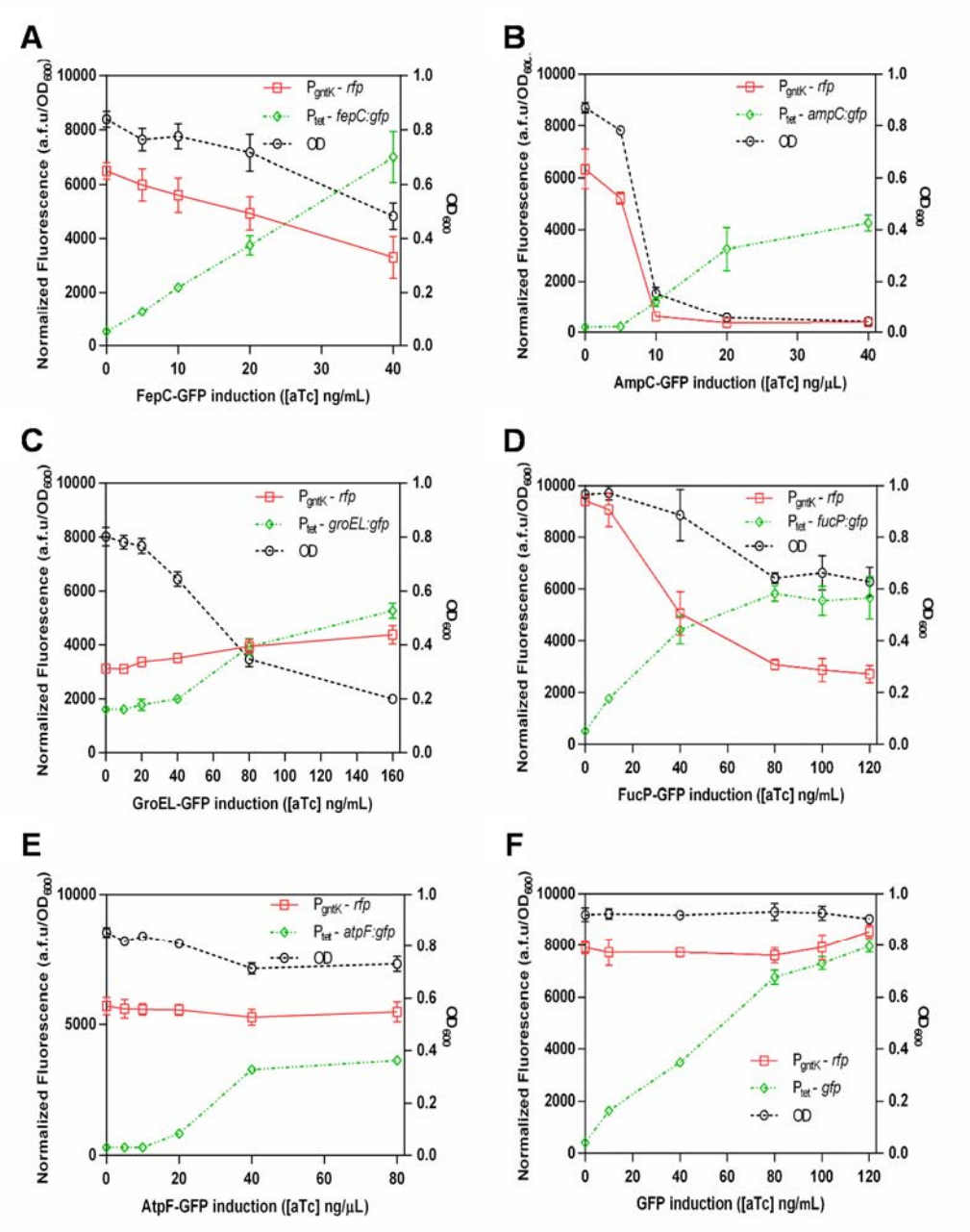

Figure 4-4: PgntK response to overexpression of various proteins.
PgntK is repressed by toxic overexpression of the membrane protein FepC (A), but not by the toxic overexpression of cytoplasmically localized GroEL(C). Additionally, non-toxic overexpression of Atp-F does not result in repression of PgntK (E). PgntK is repressed by toxic overexpression of the periplasmic protein AmpC (B), and the membrane transporter FucP (D). Overexpression of the non-toxic cytoplasmic control protein, GFP, does not change PgntK activity (F). Cells containing the PgntK-rfp plasmid were transformed with plasmids containing genes encoding the representative proteins translationally fused to GFP under the expression control of the inducible Ptet promoter. The activity of PgntK was monitored through RFP fluorescence. Data was collected 6 hours after induction. Error bars denote one standard deviation, n=4.

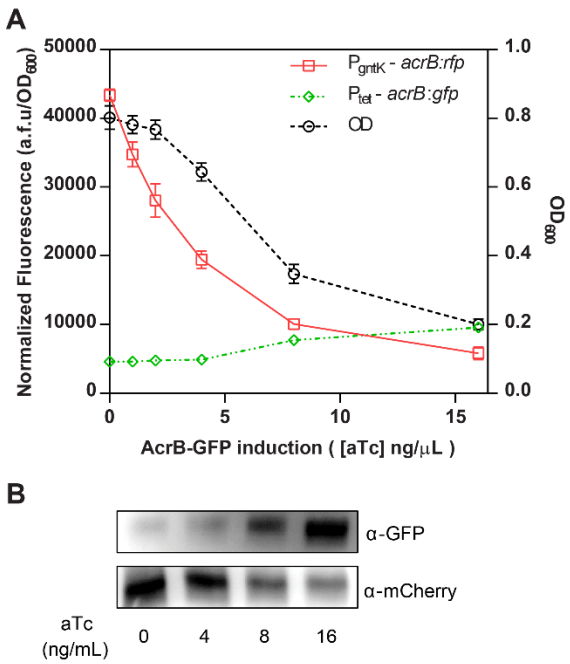

Figure 4-5: In a feedback loop, PgntK dynamically regulates expression of AcrB.
P_{gntK}-controlled expression of AcrB is responsive to total AcrB levels as shown by fluorescence (A) and subsequent western blots against the fluorophores (B). Cells containing the P_{gntK}-*acrB:rfp* plasmid in a Δ*gntK* background strain were transformed with plasmids containing *acrB:gfp* under the control of the inducible P_{tet} promoter and the expression of AcrB from the two plasmids was monitored with RFP and GFP fluorescence. Data was collected 6 hours after induction. Bands on western blots were cut at the approximate size of the AcrB-FP fusion. Error bars show one standard deviation, n=4.

4.2.6 P_{gntK} drives optimum expression of mutant AcrB expression for minimizing butanol toxicity

To determine whether P_{gntK} could control levels of an efflux pump to increase overall tolerance to *n*-butanol, we employed AcrBv2, a variant of AcrB that we previously engineered to act on *n*-butanol [38]. Cells containing a plasmid expressing AcrBv2 with the wild-type accessory proteins AcrA and TolC have increased growth in media containing toxic concentrations of *n*-butanol compared to controls. We replaced the P_{bad} promoter governing the expression of the operon with P_{gntK} and observed cell growth in media containing 0.7% *n*-butanol. In wild-type BW25113 cells, strains containing the P_{gntK}-*acrBv2* plasmid performed as well as those containing the P_{bad}-*acrBv2* construct that was optimized for tolerance in the absence of inducer (data not shown). This was not surprising, as our previous study reported that even a small amount of overexpression of AcrBv2 from the P_{bad} promoter decreased tolerance in *n*-butanol [38]. However, in the Δ*gntK* knockout strain, in which the repression range of the P_{gntK} promoter to AcrB-induced stress is greater, a slight increase in tolerance to *n*-butanol was observed when P_{gntK} was used to control AcrBv2 expression, as compared to the optimal expression from the inducible vector (Figure 4-6A). Notably, in the BW25113 Δ*gntK* strain, leaky expression of AcrBv2 from the P_{bad} promoter does not yield the highest tolerance to 0.7% *n*-butanol as it does in the wild-type strain. We performed end-point growth assays to determine the optimal inducer concentration for AcrBv2 from the P_{bad} promoter in BW25113 strain and found it to be approximately 0.002% arabinose (w/v) (Figure 4-6B). This is a very small level of induction, yet it yields a statistically significant difference in *n*-butanol tolerance compared to no induction (0.56±0.02 and 0.51±0.01 OD_{600} after 6 hours of growth respectively, p-value <0.05 by Student's t-test). Expression from P_{gntK} in the same strain in media containing 0.7% *n*-butanol results in even higher growth (0.58±0.02 OD_{600} after 6 hours, p-value <0.05

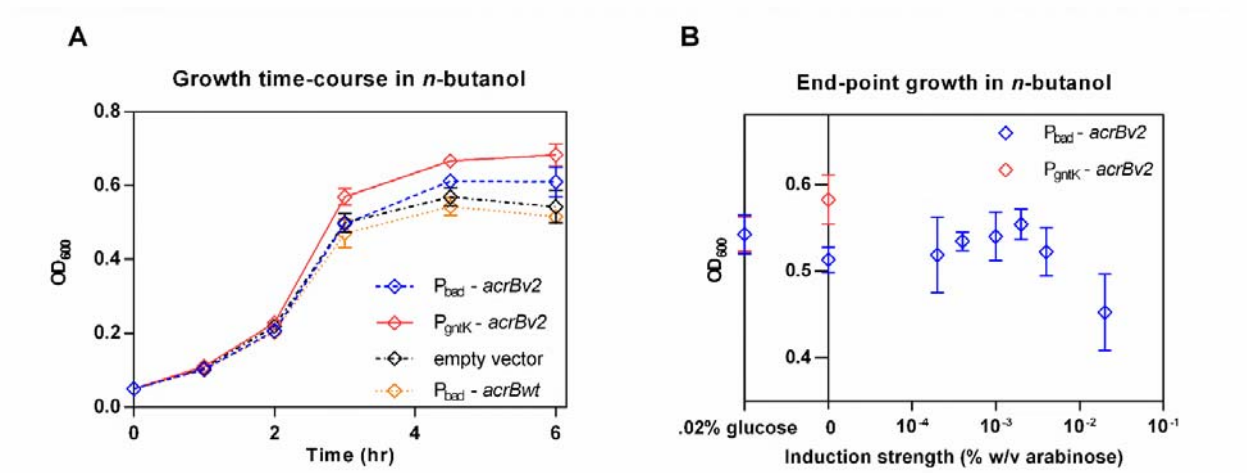

Figure 4-6: PgntK expression control of AcrBv2 confers increased growth of ΔgntK strains in n-butanol.
(A) P_{gntK}-controlled AcrBv2 strains grew faster and to higher ODs compared to the previously expression optimized P_{bad}-*acrBv2* strains. Cells containing indicated plasmids were grown in LB media with 0.7% (w/v) *n*-butanol. (B) End-point (6 hrs) OD_{600} measurements of the BW25113 Δ*gntK* strain containing *acrBv2* under the control of the P_{gntK} or P_{bad} promoters in 0.7% *n*-butanol shows the need for tight regulation of induction levels. Highest tolerance occurs at 0.002% w/v arabinose in the strain with the inducible vector, while expression from P_{gntK} confers the maximum density without the need of inducers. When grown on 0.02% glucose, cells containing either plasmid showed no difference in growth as both promoters are catabolically repressed. The OD_{600} axis starts from 0.35 to better highlight the small optimal concentration window. Error bars show one standard deviation, n=3.

compared to no induction from P_{bad} promoter). No optimization of growth conditions or inducer concentration was required to achieve this result. We further compared the expression of AcrB in these strains by western blot and found expression from P_{gntK} closely matched the most optimal induction strength from the P_{bad} promoter. In the Δ*gntR* knockout strain, P_{gntK} performed worse than leaky P_{bad} expression, presumably due to the high basal expression levels in that strain (Figure 4-3B).

4.2.7 P_{gntK} driven AcrBv2 increases *n*-butanol production in *E. coli*

Efforts to engineer efflux transporters for increased secretion of small molecules do not often translate to increased production of the small molecule during fermentation[95]. *N*-butanol titers are typically on the order of 1 g/L, while toxicity arising from *n*-butanol is prevalent at concentrations four to ten times greater than that. When titers are low, the toxicity associated from expressing butanol secreting pumps may overshadow any benefits conferred by efflux, and it is imperative to tightly control expression of the pumps. To this end, we tested our system containing the gene encoding the AcrBv2 mutant under the control of the P_{gntK} promoter in strains that also contain the butanol production plasmids from Bond-Watts et al.[53]. To make our pumps compatible and independent from the butanol production system, we placed *acrB* or *acrBv2* along with the genes encoding accessory proteins *acrA* and *tolC* under the control of the P_{tet} or P_{gntK} promoter in a pSC101 origin plasmid into BW25113 *ΔgntK E. coli* strains. Strains expressing wild-type AcrB and non-induced AcrBv2 strains showed no increase in butanol production over RFP control plasmids (Figure 4-7). However, optimized expression of the P_{tet}-AcrBv2-AcrA-TolC vector

(2 ng/mL aTc) increased butanol production by 35%. As with the tolerance phenotype, cells containing the AcrBv2 variant under the control of the P_{gntK} promoter showed an improvement in *n*-butanol titer similar to that gained by optimizing expression from the inducible promoter. No significant growth defects or advantages were observed in strains overexpressing AcrBv2 despite the increase in titer. (data not shown)

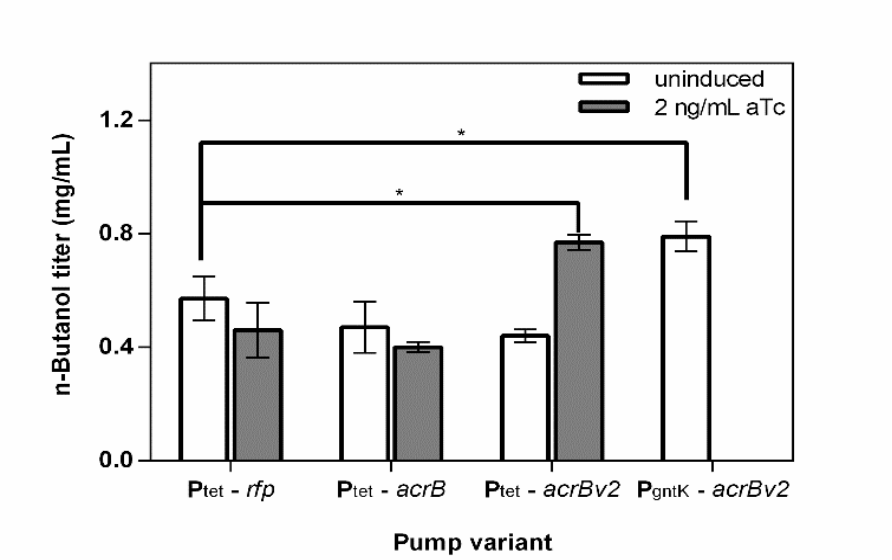

Figure 4-7: *N*-butanol production is increased in strains containing AcrBv2
BW25113 Δ*gntK* cells transformed with *n*-butanol production pathways as well as a vector encoding efflux pump variants or the RFP control were allowed to produce *n*-butanol for 72 hours. Final titers were measured by HPLC. The presence of AcrBv2 increases titer only when proper expression levels are used, while P_{gntK} driven AcrBv2 produces maximum titer without any optimization. Note also the decrease in titer in cells overexpressing the wild-type AcrB, presumably due to energy loss or toxicity from the pump not specific for *n*-butanol. * indicate statistically significant difference by Student's t-test ($p<.05$). Error bars show one standard deviation, n=3.

4.3 Discussion

We found that the native *E. coli* promoter for the *gntK/U* gluconate utilization operon responds to toxicity from overexpression of the multidrug exporter, AcrB, and its mutant acting on *n*-butanol. This promoter decreases expression in response to the stress of membrane protein overexpression. Moreover, when placed in a negative-feedback loop, the promoter controls membrane protein expression to optimize growth. We demonstrated the utility of this system by placing P_{gntK} in control of the gene encoding the *n*-butanol-secreting AcrB mutant, AcrBv2. The strains harboring this genetic circuit exhibited *n*-butanol tolerance similar to those for which AcrBv2 expression was optimized by inducer titration. Thus, employing the P_{gntK} promoter to control efflux transporter levels can minimize the need for use of small-molecule inducers and eliminate the need to experimentally fine-tune expression control.

Furthermore, P_{gntK} showed decrease in activity in response to overexpression of a number of other toxic membrane and periplasmic proteins, but not to non-toxic overexpression of membrane proteins, or toxic cytoplasmic proteins. This indicates that P_{gntK} is likely responding to a global membrane stress. Interestingly, overexpression of GroEL decreases σ^{32} stability, and we noticed a slight increase in P_{gntK} activity in response to GroEL overexpression. This suggests that P_{gntK} repression may be mediated by general heat-shock response from either σ^{32} or the known response to membrane stress σ^{E}. Given that the promoter has such a ubiquitous response to membrane protein overexpression stress, it is possible that P_{gntK} could be used in applications where membrane protein expression has to be regulated to minimize toxicity. For instance, P_{gntK} can be used in high titer expression of heterologous membrane proteins for biotechnology or research applications such as crystallography.

P_{gntK} control of AcrB production to reduce *n*-butanol toxicity was most pronounced in a Δ*gntK* strain, likely due to the higher dynamic expression range observed in this strain. This response did not carry over to the Δ*gntR* strain despite an even higher dynamic expression range, likely because of the higher expression level under repressing conditions in this strain. The basal expression range can be tuned independently, however, by altering the translation efficiency through changes in the ribosome binding site. This gives P_{gntK} more flexibility depending on the target protein for which expression is to be optimized.

Finally, P_{gntK} is catabolically repressed by the presence of glucose. This gives it an advantage in expression of efflux transporters in fermentation strains, as transporter function is not required until late in the fermentation when product concentrations are high. In this scheme, the transporters are not using a large amount of energy early on in the fermentation to secrete non-toxic amounts of the product. We directly tested this approach in the proof-of-concept production of *n*-butanol. The strain in which P_{gntK} controlled the expression of AcrBv2 had the highest *n*-butanol titer without the use of a potentially costly small molecule inducer. Furthermore, this increase in *n*-butanol production did not require meticulous optimization of expression, something that may

take large resources in other membrane transporter systems, particularly those that utilize more than one efflux transporter. To our knowledge, this is the first time that dynamic regulation of an efflux transporter has been used to increase tolerance to and production of a biofuel in cells.

4.4 Methods

4.4.1 Strains and growth conditions

. All cells were grown on lysogeny broth (LB) media unless otherwise noted and supplemented with appropriate antibiotic (50 ng/mL kanamacyn, 35 ng/mL chloramphenicol, 50 ng/mL carbenicillin). Cells were incubated at 37°C and when grown in liquid media, shaken at 215 rpm. When noted, cell culture densities were monitored by the absorbance at 600 nm OD_{600}.

4.4.2 Pstress library creation

Genes that respond to envelope stress were identified from [100]. To be considered, the gene had to have at least a two-fold increase or decrease in expression due to stress, and respond to no more than three of the stresses. The 500 bp regions upstream of the gene or the operon containing the gene were amplified by PCR using primers with EcoRI and BamHI restriction enzyme sites on the 5' and 3' ends of the primers, respectively. The amplified segments were digested by EcoRI and BamHI restriction enzymes and ligated with T4 Ligase with pBb BglBrick vectors [107] cut with EcoRI and BglII containing the *mcherry* gene, a kanamycin resistance gene, and the p15a origin of replication. All enzymes were obtained from New England Biolabs (Ipswich, MA). The promoters were placed between a P_{tet} promoter and the *mcherry* gene for convenience in library construction, but all further characterization experiments were done with versions of the vector in which the P_{tet} promoter and the *tetR* gene had been removed.

4.4.3 Knockout strain construction

Knockout strains were obtained from the Keio collection. Antibiotic cassettes were removed using protocol developed by Datsenko and Wanner [75]. Briefly, strains obtained from the Keio knockout collection [103] were transformed with the pKD46 plasmids and maintained at 30°C. Cells were grown overnight and then diluted to 0.1 OD_{600} and grown for ~2 hours until 0.4-0.6 $OD_{600.}$ The λ red recombinase was induced with 10 mM arabinose for 4 hours. Cells were then moved to 37°C to cure the pKD46 plasmid and a small aliquot plated on LB agarose plates. Colonies were screened for the inability to grow on kanamycin or ampicillin and the cassette removal confirmed by sequencing of genomic DNA prep.

4.4.4 Fluorescent reporter measurements of promoter activity

Cells were transformed with indicated plasmids and grown overnight. The cultures were then diluted 1:100 and grown until reaching an OD_{600} of 0.4-0.5. The inducers arabinose (ara) or anhydrous tetracycline (aTc) were added at indicated concentrations. After 6 h, 200 μL aliquot of culture were placed in a 96-well plate and the fluorescence

emission for GFP (485/525), RFP (585/640), and the absorbance at 600 nm were recorded on a Tecan Ininifty II microplate reader (Tecan, San Jose, CA).

4.4.5 Western blotting

Cultures were prepared following the same protocol as for the fluorescent reporter assay, and samples were collected at 6 h post-induction. At this point, cells were normalized to 1 OD_{600}/mL, and centrifuged at 5000xg for 5 min. The supernatant was discarded and cells were lysed by resuspending in 100 µL 0.1% octylthioglucoside solution (Thermo Fisher). The insoluble fraction was collected from the pellet of the lysate centrifuged at 12000xg for 10 min. Western blotting was performed as previously described, but with some changes [80]. Briefly, the samples were resuspended in 100 µL Phosphate Buffered Saline (PBS) and mixed with SDS loading buffer containing 2-mercaptoethanol (final concentration loading buffer, 1x). The samples were incubated in a heat block for 2 min at 95°C and 12 µL of each sample was run on 7.5% acrylamide Tris-glycine gels. Proteins were transferred to a polyvinylidine fluoride membrane (Immobilon-P, Millipore) using the Trans-Blot SD Semi-Dry Transfer Cell (Bio-Rad). The membranes were blocked in 5% (w/v) nonfat dry milk/TBST buffer (20mM Tris-HCl, 150 mM NaCl, 0.05% Tween-20, to pH 7.5) at room temperature for 1 hour. The membranes were incubated with primary antibodies diluted in 1% milk/TBST at 4°C temperature overnight. The following primary antibodies were used: monoclonal rat anti-mCherry (Life Technologies), and monoclonal mouse anti-GFP (Sigma).

After washing in TBST, the membranes were incubated with secondary antibodies diluted in 1% milk/TBST at room temperature for 1 hour. The following secondary antibodies were used: Stabilized Peroxidase Conjugated Goat Anti-Mouse, H+L (Thermo Scientific), and Stabilized Peroxidase Conjugated Goat Anti-Rat, H+L (Thermo Scientific). After washing, proteins were detected using the SuperSignal West Femto Chemiluminescent Substrate (Thermo Scientific) and images captured with a ChemiDoc XRS+ imaging system (Bio-Rad).

4.4.6 Growth assay in *n*-butanol

Cells were grown overnight in liquid media and diluted to an OD_{600} of 0.05. 10 mL of cell culture was placed in screw-cap tubes to avoid loss of solvent due to volatility. *N*-butanol was added at indicated concentrations and the culture vortexed for 3 s to mix the solvent into solution. Absorbance at 600 nm was read on a Genesys 20 spectrophotometer (Thermo Fisher, Waltham, MA) through the glass tubes without unscrewing the cap.

4.4.7 *N*-butanol production

BW25113 Δ*gntK* cells were transformed with butanol production plasmids (pBT33-Bu1, pCWOri-ccr.adhE2) through the RbCl competency method [108]. The cells were consequently made competent again. P_{tet}-*acrBv2*, P_{tet}-*mcherry*, P_{gntK}-*acrBv2* or empty vector plasmids were transformed into the cells and colonies picked for overnight growth in LB. After overnight growth, cells were subcultured 1:100 to 2xYT media containing the appropriate antibiotics and 1.5% w/v glucose and grown to an OD_{600} of 0.5. Cultures were transferred to screw-cap flasks to avoid butanol evaporation, and were then induced for *n*-

butanol production by the addition of 1 mM IPTG and 0.2% w/v arabinose. Where appropriate, efflux pump expression was also induced by the addition of 2 ng/mL anhydrous tetracycline (aTc). Cultures were then grown at 30°C for 72 hours. Every 24 hours the OD_{600} of the culture was measured and 1.5 mL was centrifuged at 10000xg for 10 min. 1 mL of the supernatant was collected and stored at 4°C in GC vials for liquid chromatography analysis. After 24 hrs from initial induction, an extra 1% w/v glucose was added to the culture.

4.4.8 *N*-butanol concentration quantification

Butanol concentration was assessed by HPLC. 10 µL of the samples were injected onto an Rezex RFQ Fast Acid H+ (8%) (100 x 7.8 mm, Phenomenex, Torrance, CA) column and analyzed at 55 °C on a 1200 series liquid chromatography instrument equipped with a refractive index detector (Agilent Technologies, Santa Clara, CA). Elution was performed with 5 mM sulfuric acid at a flow rate of 1.0 mL/min.

Chapter 5 - Active transport of molecular farnesene in Saccharomyces cerevisiae

5.1 Background

The search for more environment-friendly processes brings microbial biochemical production to the forefront of scientific research. State-of-the-art research focuses on the production of next-generation biofuels that resemble current gasoline, diesel, and jet fuels [87,109,110]. Also in demand are alternative routes to chemicals currently derived from petroleum[111]. Pathways to microbial production are established or underway for a variety of target molecules, but investigations into efficient recovery of the cellular product lags. In particular, there is a need to understand and enhance the transport processes involved in moving product from the cytosol to the growth media and, in some cases, into an extractive phase. Hydrophobic products, such as oils, require cost-intensive methods to recover product that remains in the intracellular milieu and benefit especially from an examination of transport processes.

Organisms that naturally produce large amounts of oil-like molecules typically store the oil inside the cells. In commercial biochemical production, however, it is critical to accumulate the product extracellularly at quantities sufficient to compete in the market place. This becomes even more essential for biofuel and commodity biochemical production. Experimental evidence indicates that transport limitations exist[112,113], giving rise to difficult-to-recover intracellular product that slows the path to commercialization of highly hydrophobic molecules.

In this work, we focus on farnesene as a model for the multitude of oil-like compounds biochemically produced in microbes. Farnesene is an excellent candidate for monitoring hydrophobic molecule transport due to its low solubility in water and it is one of the few oil compounds to be microbially produced at large scale. The isoprenoid farnesene is a C_{15} unsaturated hydrocarbon (Figure 5-1A). It is an excellent substitute for diesel and jet-fuel, and serves as a precursor for surfactants, cosmetics, lubricants, and polymers. It is a highly hydrophobic, essentially water-insoluble oil with physical properties that raise challenges for cost-effective production in microbes. Farnesene is produced in bacteria and yeast from precursors isopentenyl pyrophosphate and dimethylallyl pyrophosphate[114]. These precursors are generated from the 2-C-methyl-D-erythritol-4-phosphate and mevalonate pathways in bacteria and yeast, respectively[115]. Farnesyl diphosphate is the condensation product of these two precursors; farnesene synthase converts it to farnesene. It is currently unknown if farnesene synthase produces farnesene in molecular form, or releases it directly into lipid droplets of cellular origins.

Fuel-like molecules such as farnesene collect as a free phase in the extracellular space. Transport mechanisms for cellular efflux are unknown. Notably, accumulation of farnesene increases when a hydrophobic sink is present [112,113]. The fact that overlays of extraneous oil increase supernatant collection of farnesene[116] is *prima facie* evidence of the importance of transport limitations. Evolved metabolic fluxes continue to increase,

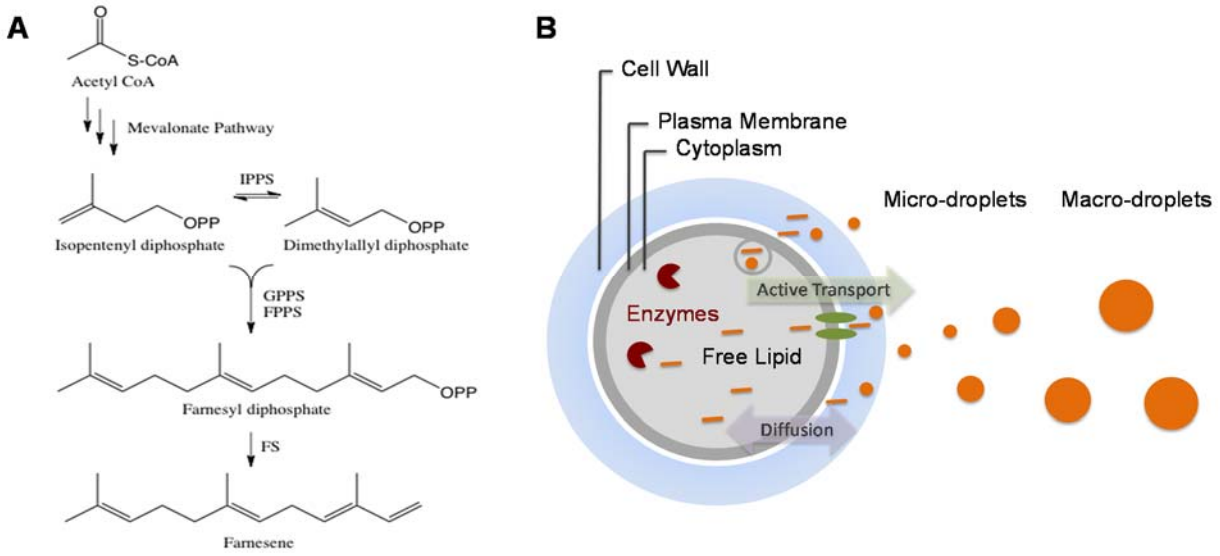

Figure 5-1 Schematic of farnesene production and transport.
(A) Metabolic pathway towards the production of farnesene in yeast. IPPS, isopentenyl diphosphate isomerase; GPPS, geranyl diphosphate synthase; FPPS, farnesyl diphosphate synthase; FS, farnesene synthase. Adapted from Peralta-Yahya *et al.* [115]. (B) Schematic of the possible routes of farnesene transport out of the cell. Actuve transport can create a gradient of molecular farnesene which promotes droplet formation out of the cell. Inside the cell, Lipid Droplets, and other lipid-rich vesicles can also sequester farenesene. Both the plasma membrane and the cell wall function as diffusion barriers, but due to the large droplet size, only the molecular farnesene is likely to diffuse in and out of the cell.

further exacerbating these limitations. Thus enhanced cellular efflux will improve overall process economics. Further, increased efflux rates reduce biochemical accumulation within the cells, thereby minimizing product toxicity[30,38]. We chose to study farnesene transport in *S. cerevisiae* as it has become the favored organism for industrial microbial production. Additionally, farnesene titers in yeast are significantly higher than in bacteria making transport limitations more apparent.

The chemical in the aqueous broth is at or above the molecular solubility limit. Accordingly, a possible transport path is by active transport across the plasma membrane either via molecular transporters or via vesicular release and then passive diffusion through the cell wall, followed by nucleation and coalescence into a free-oil phase (Figure 5-1B). This hypothesis is consistent with the observed role of hydrophobic sinks in enhancing extracellular fuel collection.

In this chapter we highlight the prediction of active transport in farnesene-producing yeast through the extension of the kinetic transport model developed earlier. We then utilize a dye-based farnesene detection system to monitor intracellular farnesene levels and show that active transport of farnesene is indeed native to *S. cerevisiae*. Finally, we identify two of the transporters responsible for farnesene transport and also parse out the intracellular localization of farnesene.

5.2 Results

5.2.1 Extension of kinetic model to immiscible products

To understand what role transporters play in the transport of farnesene and other hydrophobic molecules, we extended our kinetic transport model to include the creation of a second phase. As with the transport of polar molecules, diffusion and active transport across the membrane can be modeled respectively by the permeation of the molecule through the membrane and a Michaelis-Menten type reaction of transport enzymes secreting molecular farnesene from the cytoplasm to the outside of the cell. An additional term is added for the transport of farnesene from the broth into the extracting phase (e), represented by the flux, J_{eb}, such that the overall mass balance equations are as follows:

$$V_c \frac{dC_c}{dt} = V_c r_m - A_c(J_{ac} + J_{diff}) \tag{5-1}$$

$$V_b \frac{dC_b}{dt} = A_c(J_{ac} + J_{diff}) - A_e J_{eb} \tag{5-2}$$

$$V_e \frac{dC_e}{dt} = A_e J_{eb} \tag{5-3}$$

We also modified the parameters of the equation to represent the farnesene-yeast system better. For example, the diffusive flux increased severely due to higher partition coefficient (~10^7) of farnesene compared to primary alcohols. Since no kinetic data was available for any transporter in yeast that secreted hydrophobic molecules, we chose to model active efflux with parameters from the *E. coli* AcrA-AcrB-TolC system. We did, however, increase the expected number of transporters present in proportion to the increase in cell membrane area for yeast cells compared to *E. coli*. The solution of these expressions at steady state once again implies that the concentration gradient created by active transport depends only on the specific activity of the transporters and their numbers inside the cells.

$$\Delta C = (C_b - C_c) \propto \frac{\Gamma_t \nu_{max} \delta}{KD} \tag{5-4}$$

This result is crucial: it shows that the extracellular concentration of farnesene is higher than that inside the cells with active transport. Using known values for the permeability of farnesene across the lipid bilayer, and approximating the activity of a putative transporter as similar to that of the bacterial transporter AcrB, the value of $\frac{\Gamma_t \nu_{max} \delta}{KD}$ is only 90 μM. This concentration difference is significant, however, when the nucleation of the farnesene microdroplets is considered.

Accumulation of molecular farnesene in the broth is given by:

$$V_b \frac{dC_b}{dt} = A_c(J_{ac} + J_{diff}) - A_e J_{eb} \tag{5-5}$$

Molecular farnesene, however, does not simply partition into a secondary free phase. Farnesene must first undergo droplet formation, most likely through a nucleation process. According to classical nucleation theory (Kashchiev 2003), the nucleation rate (number of nuclei/volume/time) is given by:

$$J_{nuc} = Ae^{-\left[\frac{\Delta G}{k_B T}\right]} \tag{5-6}$$

Where A is the pre-exponential factor, k_B is the Boltzmann constant, T is the temperature, and ΔG is the free energy for nucleus formation. For nucleation due to supersaturation:

$$\Delta G = \frac{16\pi {v_s}^2 \gamma^3}{3\left[k_B T \ln(\frac{C}{C_{sat}})\right]^2} \tag{5-7}$$

Where v_s is the molecular volume, γ is the surface tension between the droplet and water (assumed to be equal to the surface tension of typical oils and water) and C_{sat} is the molecular saturation concentration of farnesene.

The pre-exponential factor A for this reaction is very difficult to quantify either through theoretical calculation or experimentally[117,118]. A large range can be obtained from literature (10^{20}-10^{29} nuclei/mL-sec)[118], but in even the smallest value yields a rate considerably larger than the rates of production or transport across the cell membrane discussed earlier. The overall balance on the molecular farnesene inside the broth is then given by:

$$V_b \frac{dC_b}{dt} = A_c \left[\frac{KD}{\delta}(C_c - C_b) + \Gamma_t v_{max}\right] - \frac{v_{nuc}}{v_s} V_b \frac{A}{N_A}\, e^{-\left[\frac{16\pi {v_s}^2 \gamma^3}{3k_B T\left[k_B T \ln\left(\frac{C_b}{C_{sat}}\right)\right]^2}\right]} \tag{5-8}$$

Where N_A is Avogadro's number, and v_{nuc} is the critical minimum volume of a newly formed nucleus, assumed to be a sphere of radius $r_c = \frac{2v_s\gamma}{k_B T \ln\left(\frac{C_b}{C_{sat}}\right)}$. Because of the dominating strength of the pre-exponential factor A, any supersaturating conditions give almost instantaneous nucleation. This conclusion implies that active transport is a mechanism for limiting the nucleation of farnesene droplets to the outside of the cell. Since $C_b > C_c$ as demonstrated in Equation (5-4), nucleation occurs in the broth while the concentration of molecular farnesene in the cells is maintained below C_{sat}. Fast nucleation keeps the molecular concentration of farnesene at saturation outside of the cells such that $C_b \cong C_{sat}$. Increasing the concentration gradient ensures that minimal farnesene is left inside the cells where it may be difficult to recover from in downstream processing. In addition to decreasing the concentration of farnesene inside the cells, an increase in efflux results an increase in the concentration of molecular farnesene over saturation in the broth. This leads to a decrease in the critical radius of the nucleated droplets present outside of the cells. A decrease in nucleation size contributes to faster diffusion of the

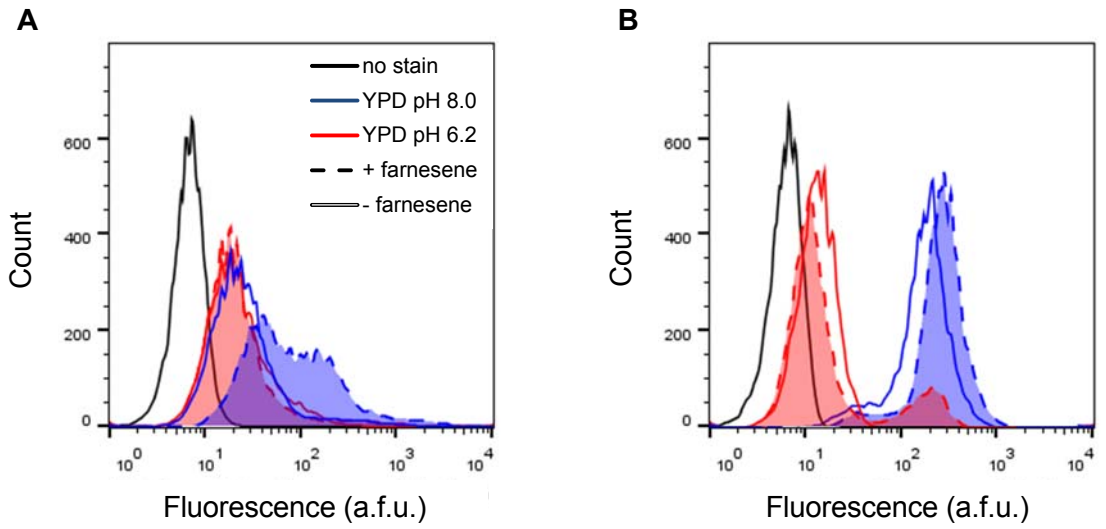

Figure 5-2 pH-dependent efflux of farnesene in yeast
Wild-type *S. cerevisiae* were grown in high (blue) or low (red) pH YPD media. Cells were also grown with (dashed outline, filled in) and without (solid outline) the presence of farnesene. Cells were then subjected to Nile Red straining protocol and fluorescence recorded by flow cytometry. Black line represents no-straining control (A) Cells take up farnesene only at high pH. (B) Cells that were grown in the presence of farnesene at high pH (blue, filled from (A)), are then grown in fresh media. Moving cells to acidic media restores efflux, while maintaining high pH causes no release of farnesene, even if no exogenous farnesene is present.

droplets through the cell wall and enhances transport of the overall system. Such insights were not obvious without a formulation of this guiding kinetic model.

5.2.2 High extracellular pH disrupts increases farnesene accumulation inside the cell

We devised a method for identifying intracellular farnesene concentrations in real time without perturbation to the cells. We utilize the fluorescent dye Nile Red that associates with hydrophobic molecules and is useful for labeling lipids[119]. We grew wild type (i.e., non-farnesene producing) *S. cerevisiae* in the presence of exogenous 0.8 M suspended aqueous farnesene, a concentration higher than saturation and similar to that found in a large-scale fermentation, for 5 h starting at mid-log phase. The cells were then stained with Nile Red, washed, and assessed by flow cytometry (Figure 5-2). Only 1% of cells exhibited higher than background fluorescence associated with intracellular concentrations of farnesene. Therefore, since passive transport is bidirectional, this results supports our assertion that active efflux must equal or exceed any passive influx in wild type *S. cerevisiae*. These results were confirmed by analyzing a sample of cells by fluorescent microscopy; where cells incubated with farnesene and Nile Red in regular, pH 6.2 media did not appear significantly more fluorescent than the control population, while those grown in high pH media showed increased fluorescence.

We next performed a test to assess one form of active transport. Since mechanisms that depend on a proton gradient across the cell membrane can be disrupted or even reversed in high pH media, we grew cells in the same media (containing farnesene) described above except titrated to a pH of 8.0. The cells grown this way showed an increased uptake of farnesene (Figure 5-2A).

5.2.3 High extracellular pH disrupts farnesene efflux

High extracellular pH could cause intracellular farnesene accumulation in one of two ways: 1) basic pH conditions could increase the rate at which farnesene is able to enter the cell or 2) high pH could disrupt farnesene efflux from the cell that naturally dominates transport. To assess which mechanisms are occurring in our system, we isolated cells grown in basic media with farnesene, and thus containing intracellular farnesene, and moved these cells to fresh basic or acidic media containing no farnesene. If high pH increases farnesene uptake while the cells have no natural efflux, then the cells should maintain intracellular farnesene concentrations regardless of media pH after loading. If high pH increases farnesene uptake, but some basal efflux mechanisms exist, then when cells loaded with farnesene are grown in either basic or acidic media, cellular farnesene concentrations would decrease regardless of media pH. Finally, if high pH disrupts efflux only, then after cells are transferred to media without exogenous farnesene, only cells in high pH media would maintain high intracellular concentrations of farnesene. This is the outcome that is supported by Nile Red fluorescence data of cells containing intracellular farnesene that are transferred to media without farnesene. Restoration of the proton gradient results in efflux of farnesene (Figure 5-2B).

5.2.4 Proton gradient and ATP mediated transport are involved in farnesene efflux

To further confirm that active transport was responsible for farnesene efflux in yeast, we performed the fluorescent labeling assay while growing cells in the presence of transport inhibitors. Diethylstilbestrol (DES), an H^+-ATPase inhibitor, has been shown to neutralize the plasma membrane proton gradient without affecting other ATP-related processes[120]. Similar to the experiment with high pH media, the addition of DES to regular YPD media with exogenous farnesene present increased farnesene accumulation in the cells. Furthermore, the addition of vanadate, an ATPase and ABC transporter inhibitor, also increases intracellular accumulation of farnesene. This result indicates that ATP-driven transport, in addition to H^+ gradient driven transport, is responsible for transport of farnesene (Figure 5-3A). Growing cells in basic media with addition of vanadate further increased intracellular farnesene accumulation compared to vanadate alone. Thus two different energy sources are utilized in tandem in the cell to secrete farnesene, implying that at least two active mechanisms are involved in this process. Furthermore, vanadate-mediated disruption of efflux resulted in higher farnesene accumulation than DES-mediated inhibition of efflux, indicating that perhaps the ATP-driven process is slightly more favored. We utilize vanadate induced transport inhibition with the addition of farnesene as a method to artificially load cells with farnesene in the rest of this work.

5.2.5 The native Pdr5 and Snq2 transporters secrete farnesene from the cell

Our studies indicated that an active mechanism is responsible for farnesene efflux. The specific reliance on the membrane proton gradient supports the presence of molecular transporters responsible for this efflux. Based on our modeling results, molecular active transport is sufficient for the creation of an extracellular farnesene phase without high accumulation of farnesene in the cell. We therefore expected that molecular efflux transporters must be involved in farnesene efflux, and, consequently, tested a small

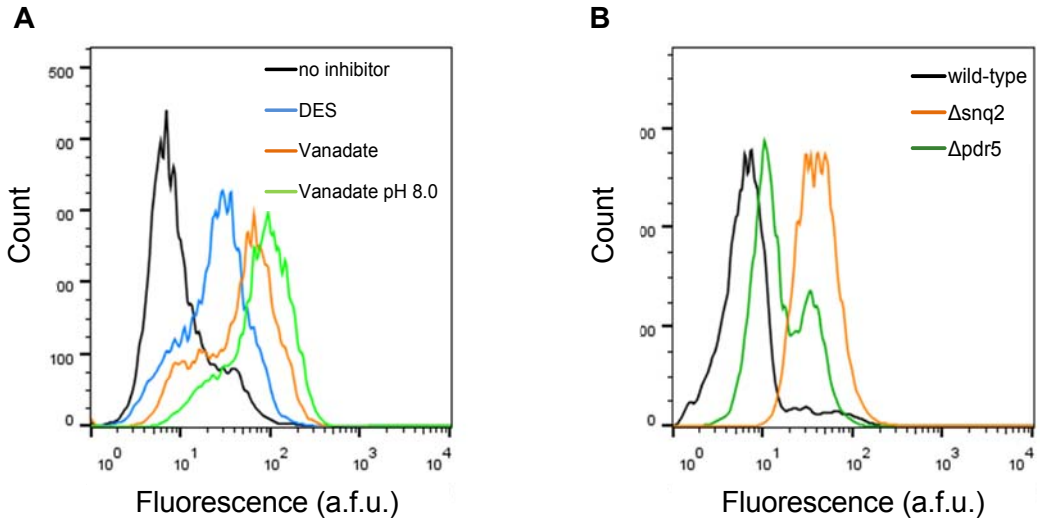

Figure 5-3 ATP-driven efflux transporter activity on farnesene
Flow-cytometry histograms of Nile Red-strained cells after growth in farnesene containing media. (A) Media was supplemented with inhibitors of the plasma membrane proton motive force (diesthylstilbestrol, DES, blue) and ATP (vanadate, orange). Disruption of either energy source decreases farnesene export. When both mechanisms are deactivated by adding vanadate to basic media, total uptake increases. (B) Strains knocked out for Snq2p (green) and Pdr5p (orange) have increased intracellular farnesene association compared to wild-type cells.

library of known transporter knockouts on their ability to efflux exogenously added farnesene. Knockout strains were subjected to the accumulation assay by adding farnesene in acidic YPD media. *SNQ1Δ*, *PDR15Δ*, *YOR1Δ*, and *TPO1Δ* cells showed similar staining as wild-type cells. The transporters encoded by these genes are known to act on a variety of substrates with varying levels of hydrophobicity yet their absence did not increase farnesene accumulation inside the cell. However, *SNQ2Δ* and *PDR5Δ* strains showed an increase in farnesene uptake compared to wild-type cells (Figure 5-3B). Snq2p and Pdr5p are ATP-driven transporters that have been implicated in transport of sterols and have some overlapping substrate specificities[121], yet no activity on isoprenoids has been observed before. Since the increase in uptake fluorescence in either mutant was not as high as when all ATP-based transport is inhibited, we expect that other pumps may be aiding in transport as well. Similar studies of more comprehensive transporter knockout libraries may yield additional candidates for transport of farnesene.

5.2.6 Farnesene accumulates within lipid droplets in the cell

The Nile Red staining assay for farnesene accumulation relies on the fact that Nile Red fluoresces in a hydrophobic environment. In an aqueous solution, Nile Red is completely quenched, and any fluorescent signal detected indicates a hydrophobic environment present in the cell. Since cells grown in the absence of exogenous farnesene and stained with Nile Red produce low yellow fluorescence signal by flow cytometry, any farnesene that does accumulate in the cell must be present in sufficient quantities to change the local hydrophobic environment. Therefore, the flow cytometry data indicate

that farnesene is able to accumulate into droplets inside the cells. We reasoned that farnesene is most likely to partition into lipid bodies, in which cells store other hydrophobic molecules including sterols and triacylglycerols. To test this idea, we applied the farnesene loading protocol using vanadate to inhibit efflux and then imaged the cells stained with Nile red under a microscope.

Industrial production strains are often heavily divergent from their laboratory parents. Since it is likely that strains engineered to produce the highest amount of farnesene will undergo genomic changes in lipid production and storage, we sought to look at intracellular farnesene accumulation within production-relevant strains. We thus transitioned to the *S. cerevesiae* strain Y15788 from Amyris, Inc. This strain has been engineered with the farnesene production pathway and optimized through multiple mutagenesis and screens for high farnesene production when the pathway is activated.. However, the pathway is only basally expressed in YPD media, and no detectable farnesene accumulation occurs unless farnesene production pathway is induced. For this assay, we used these non-production conditions. Lipid droplets are visible in by fluorescent microscopy of the Nile Red stained cells as distinct puncta (Figure 5-4, top row). Nile Red fluorescence for these droplets is primarily confined to the red region with excitation/emission at 564nm/620nm. When exogenous farnesene is added to the cells, the fluorescence of the lipid droplets in the yellow region (488nm/545nm) increases dramatically (Figure 5-4, second row), while no other subcellular structures show increased fluorescence. This finding indicates that farnesene accumulates in lipid droplets when it is not secreted from the cell via active transport.

We then performed similar experiments on a mutant strain, Y24035, deficient in lipid droplet production. These mutants (*ARE1Δ*, *ARE2Δ*, *DGA1Δ*, *LRO1Δ*)[122] are incapable of producing sterols and triacylglycerols and do not show the characteristic red-fluorescent puncta in Nile Red stained cells (Figure 5-4, third row). Interestingly, these mutants accumulate farnesene when efflux is disrupted as well (Figue 5-4, bottom row), and the farnesene aggregates into droplets that have no polar lipids in them. This indicates that farnesene nucleates into droplets inside the cell, but will not do so if there is significant lipid environment present for partitioning instead.